Geology and Geophysics Applied to Groundwater Hydrology at Fort Irwin, California

David C. Buesch, Editor

Cenozoic Geology of Fort Irwin and Vicinity, California

By David C. Buesch, David M. Miller, and Christopher M. Menges

Open-File Report 2013–1024–C

U.S. Department of the Interior
U.S. Geological Survey

U.S. Department of the Interior
RYAN K. ZINKE, Secretary

U.S. Geological Survey
James F. Reilly II, Director

U.S. Geological Survey, Reston, Virginia: 2018

For more information on the USGS—the Federal source for science about the Earth, its natural and living resources, natural hazards, and the environment—visit https://www.usgs.gov or call 1–888–ASK–USGS (1–888–275–8747).

For an overview of USGS information products, including maps, imagery, and publications, visit https://store.usgs.gov.

Any use of trade, firm, or product names is for descriptive purposes only and does not imply endorsement by the U.S. Government.

Although this information product, for the most part, is in the public domain, it also may contain copyrighted materials as noted in the text. Permission to reproduce copyrighted items must be secured from the copyright owner.

Suggested citation:
Buesch, D.C., Miller, D.M., and Menges, C.M., 2018, Cenozoic geology of Fort Irwin and vicinity, California, chap. C *of* Buesch, D.C., ed., Geology and geophysics applied to groundwater hydrology at Fort Irwin, California: U.S. Geological Survey Open-File Report 2013–1024–C, 39 p., https://doi.org/10.3133/ofr20131024C.

ISSN 2331–1258 (online)

Contents

Figures

Tables

Conversion Factors

International System of Units to U.S. customary units

Multiply	By	To obtain
	Length	
centimeter (cm)	0.3937	inch (in.)
millimeter (mm)	0.03937	inch (in.)
meter (m)	3.281	foot (ft)
kilometer (km)	0.6214	mile (mi)

Temperature in degrees Celsius (°C) may be converted to degrees Fahrenheit (°F) as °F = (1.8 × °C) + 32.
Temperature in degrees Fahrenheit (°F) may be converted to degrees Celsius (°C) as °C = (°F – 32) / 1.8.

Datum

Vertical coordinate information is referenced to the North American Vertical Datum of 1988 (NAVD 88).
Horizontal coordinate information is referenced to the North American Datum of 1983 (NAD 83).
Altitude, as used in this report, refers to distance above the vertical datum.

Acronyms

AEM	airborne electromagnetic
JRC	joint profile and roughness coefficient
LEM	laboratory electromagnetic measurements
SI	Système International
TEM	time-domain electromagnetic
USGS	U.S. Geological Survey

Abbreviations

Ga	giga-annum (10^9 years)
Ma	mega-annum (10^6 years)

Cenozoic Geology of Fort Irwin and Vicinity, California

By David C. Buesch, David M. Miller, and Christopher M. Menges

Abstract

The geology of the Fort Irwin National Training Center in the north-central Mojave Desert, California, provides insights into the hydrology and water resources of the area. The Fort Irwin area is underlain by rocks ranging in age from Proterozoic to Quaternary that have been deformed by faults as young as Quaternary. Pre-Tertiary sedimentary, igneous, and metamorphic bedrock and Miocene volcanic and sedimentary rocks are exposed in the mountains and ridges, between which are basins containing Quaternary to Pliocene deposits. During the Miocene, in the western part of Fort Irwin, development of the Eagle Crags volcanic field resulted in a complex assemblage of lava flows, pyroclastic flow and fallout tephra deposits, and volcaniclastic sedimentary rocks that were deposited in alluvial, fluvial, and locally lacustrine environments; in the eastern part of Fort Irwin, epiclastic sedimentary rocks and minor tuffaceous rocks were deposited in alluvial, fluvial, and locally lacustrine environments. In the Pliocene and Quaternary, sandstone and conglomerate were deposited in alluvial and fluvial environments, and locally fine-grained materials were deposited in lacustrine, eolian, playa, and groundwater discharge environments. The Fort Irwin area is transected by Neogene to Holocene northwest- and east-striking (and fewer northeast-striking) strike-slip, normal, and locally thrust faults. Structural blocks between faults are broadly warped, and locally rocks adjacent to the faults are folded and sheared. Many of these faults influenced the formation or modification of basins, especially after about 11 million years, when the Eastern California Shear Zone developed in this area. The three-dimensional geologic framework produced by the late Cenozoic stratigraphic and structural history is represented by the continuity or spatial limitations of lithostratigraphic and correlative hydrogeologic properties. The continuity or limitations of rocks and properties influence how water moved (and moves) through the hydrogeologic system.

Introduction

Fort Irwin National Training Center (hereafter referred to as Fort Irwin) is located in the north-central part of the Mojave Desert, California, and is a geologically diverse area underlain by rocks ranging in age from Proterozoic to Quaternary that have been deformed by faults as recently as the Quaternary (Miller and others, 2014). Like other areas in the Mojave Desert, Fort Irwin has numerous mountain ranges and ridges (fig. 1) that expose pre-Tertiary sedimentary, igneous, and metamorphic bedrock, and Miocene volcanic and sedimentary rocks. Between these ridges are basins with Quaternary to Pliocene deposits that overlie the older rocks. Intensive geologic and hydrogeologic studies elsewhere, including surface-based and borehole-based measurements, have shown strong correlations of lithologic and hydrogeologic properties in sedimentary and volcanic rocks to infiltration and transport of water through the unsaturated zone, and to transport and storage of water in the saturated zone (Flint and others, 2001; Flint and others, 2002; Flint and others, 2006). Thus, an understanding of the rocks formed and faulted in the Fort Irwin area during the Miocene, Pliocene, and Quaternary is essential in evaluating hydrogeologic properties and groundwater resources.

The Miocene rocks in and around the Fort Irwin area have been described in some detail (Byers, 1960; Brady, 1984; Spencer, 1990a, b; Fillmore, 1993; Sabin and others, 1994; Sobieraj, 1994; Yount and others, 1994; Schermer and others, 1996; Pavlis and others, 1998; Miller and Yount, 2002). Pliocene(?) to Quaternary deposits in and around the Fort Irwin area have also been described (Yount and others, 1994; Menges and others, 2001; Miller and Yount, 2002; Miller and others, 2011; Miller, 2012). This chapter summarizes the previous studies, expands upon them with additional lithostratigraphic descriptions, and develops these relations in the context of the Fort Irwin area. A generalized geologic map of the Fort Irwin area is presented in chapter B of this report (Miller and others, 2014), and some of the descriptions and discussions are reiterated and expanded upon in this chapter because they help define the Cenozoic history of the area. Mapping and borehole studies of the Quaternary deposits revealed important relations (Miller and others, 2014; Buesch, 2018), although the geomorphology and sedimentology of these deposits is widely distributed and generally thin, and can provide clues to older rocks that might be at depth.

The Fort Irwin area, which is within the eastern California shear zone (Dokka and Travis, 1990; Spencer, 1990a, 1990b; Ford and others, 1992; Yount and others, 1994; Schermer and others, 1996; Pavlis and others, 1998; Glazner and others, 2002; Miller and Yount, 2002), is transected by a series of Neogene to Holocene northwest- and east-striking (and fewer northeast-striking) strike-slip, normal, and locally thrust faults (Miller and others, 2014). Several faults, especially east-striking faults, have displaced rocks as much as 5 to 10 kilometers [km] (Schermer and others, 1996; Pavlis and others, 1998), and some of these faults deform materials as young as Pleistocene in age. A few faults, such as the Garlock, East Goldstone, and Coyote Canyon Faults, have ruptured Holocene deposits (Miller and others, 2014).

This chapter has five main goals:

1. Describe the distribution of pre-Tertiary bedrock and Miocene, Pliocene(?), and Quaternary materials.
2. Describe the Miocene volcanic and sedimentary rocks, including possible source areas, resulting lithofacies, and generalized architecture of these rocks.
3. Summarize the Quaternary to Pliocene(?) deposits.
4. Summarize the distribution of faults and folds, and the time during which they were active.
5. Describe the lithostratigraphic and structural features in the context of hydrogeologic properties and possibly groundwater resources.

EXPLANATION

Dry lake areas

Fort Irwin Military Reservation boundary

Fault or Fault Zone—Dashed where concealed

Map abbreviations

CCF	Coyote Canyon Fault
CLF	Coyote Lake Fault
CMF	Cave Mountain Faults
EGLFZ	East Goldstone Lake Fault Zone
FIF	Fort Irwin Fault
GFZ	Garlock Fault Zone
NLF	Nelson Lake Fault
OLF	Owlshead Lake Fault
PFZ	Paradise Fault Zone
SAF	Soda Avawatz Fault
SDVFZ	Southern Death Valley Fault Zone
SMF	Soda Mountains Fault
TMFZ	Tiefort Mountains Fault Zone

Figure 1. Map of geographic locations and faults in the Fort Irwin area, California, displayed on a shaded-relief base map (adjacent page). Fault locations from Miller and others (2014).

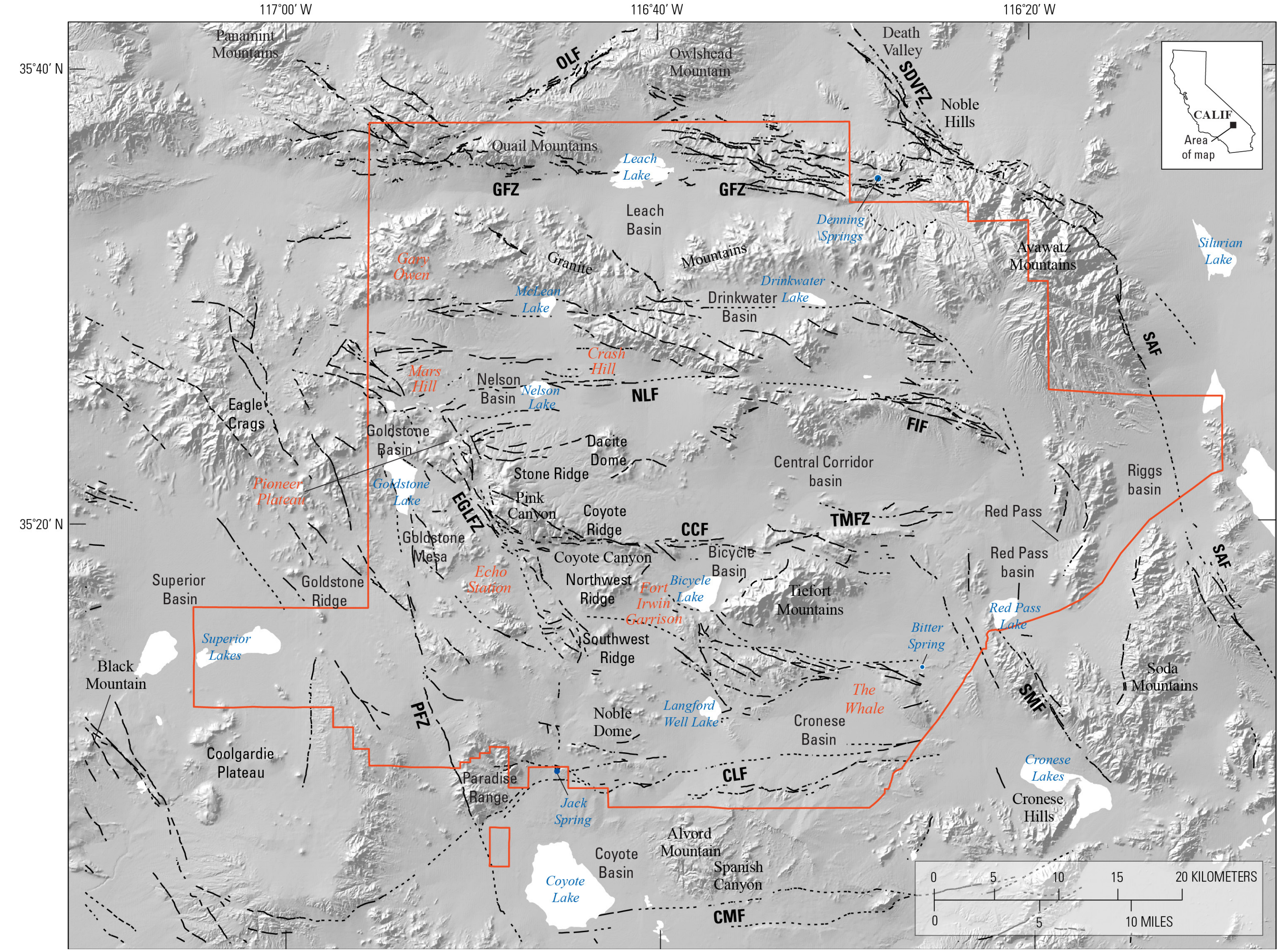

Figure 1.—Continued

Most of the location names used in this report are from published maps and literature; however, informal names have been used for numerous locations (fig. 1). Some of these informal names are based on names used by the U.S. Army or National Aeronautics and Space Administration (NASA), geomorphic basins that are coincident groundwater basins (Buesch, 2014), abandoned mining districts, or boreholes drilled as part of the 2010–12 groundwater investigations. Throughout this report, because the depths of samples and geophysical logs in boreholes were originally collected in feet, depth measurements have been converted to metric (Système International [SI]) units.

Methods

The data and relations described in this chapter are derived from several different sources. Many of the field relations are from the geologic mapping described in Miller and others (2014) and the examination of reference sections of volcanic and sedimentary rocks to establish stratigraphy and potential correlations with borehole materials (Buesch, 2018). Hand samples of selected lava flows, tuffaceous rocks, and sedimentary rocks exposed at the ground surface and selected core samples from boreholes were studied in polished thin sections for petrologic analysis. The ages are from a variety of citations that include descriptions of methods; the Mesozoic ages are primarily based on U-Pb zircon data (supplemented by K-Ar and $^{40}Ar/^{39}Ar$ data where needed), and Cenozoic ages are based on $^{40}Ar/^{39}Ar$ data with some tephrochronologic data. Data were also incorporated from a variety of geophysical techniques including analysis of resistivity from laboratory electromagnetic measurements (LEM) (Bloss and Bedrosian, 2015), field-based time-domain electromagnetic (TEM) surveys (Burgess and Bedrosian, 2014), airborne electromagnetic (AEM) surveys (Bedrosian and others, 2014), and gravity and aeromagnetic surveys (Jachens and Langenheim, 2014; Langenheim and Jachens, 2014). The geophysical techniques are described in detail in the other chapters in this report.

Lithostratigraphy

Rocks and formations described in this section have varying importance for hydrologic purposes. In general, pre-Tertiary metamorphic and granitoid rocks are described cursorily because they are not significant repositories of water. In contrast, Cenozoic (especially Miocene and Pliocene) volcanic and sedimentary rocks of Fort Irwin may be very important as reservoirs, and are described more completely. Similarly, Quaternary materials are described in moderate detail because the geomorphology and sedimentology of these deposits can provide clues to older rocks that might be at depth.

Pre-Tertiary Rocks

Metamorphic (including metasedimentary and metavolcanic) and plutonic rocks form the pre-Tertiary bedrock of the Fort Irwin area (fig. 2). These rocks are not included in the hydrogeologic modeling, other than to form the base of the model. However, these rocks have different properties that allow interpretation of gravity and magnetic data to determine the depth to bedrock, geometry of Cenozoic basins, and character of the pre-Tertiary bedrock. Distributions of these rocks are also important constraints on the structural and tectonic framework. In addition, detritus eroded from these rocks form basin-fill deposits that have some predictable properties based on the parent rocks.

Metamorphic Rocks

Metamorphic rocks in the Fort Irwin area include gneiss, schist, quartzite, marble, and metavolcanic rocks (fig. 2). The oldest metamorphic rocks are granitic gneisses dated at about 1.4 billion years [Ga] (Schermer and others, 1996; map unit “mr” of Miller and others, 2014; brown in fig. 2). These rocks are adjacent to metasedimentary rocks (map units “sl” and “ca” of Miller and others, 2014; orange and yellow in fig. 2, respectively) in a narrow belt that lies south of the Tiefort Mountains and southeast of Bicycle Lake. The metasedimentary rocks are quartzite and marble interpreted as Paleozoic miogeoclinal strata (Schermer and others, 1996; Schermer and others, 2001). Schist and quartzite (map units “sc” and “sl” of Miller and others, 2014; green and orange in fig. 2, respectively), interpreted as part of the Proterozoic Pahrump Group, lie northeast of the Tiefort Mountains. Another group of metamorphic rocks (also included in map unit “mr” of Miller and others, 2014) is found in the Bicycle Lake area, Jack Spring area, Paradise Range, and Goldstone Mining District. These strata, which have been interpreted as Paleozoic eugeoclinal rocks (McCulloh, 1960; Miller and Sutter, 1982; Schermer and others, 1996; Schermer and others, 2001; Miller and Yount, 2002), are typically dark-colored, biotite-rich schist and amphibole schist, although quartzite and marble occur as well. Remaining metamorphic rocks are felsic metavolcanic rocks covering a wide area from near the Garlock Fault, west of the Avawatz Mountains, and south to the Soda Mountains (Jennings and others, 1962); they are similar in many respects to intermediate to felsic Jurassic rocks farther south in the Cronese Hills (Walker and others, 1990) and Soda Lake (Grose, 1959) areas. These metavolcanic rocks are probably related to the Jurassic Sidewinder volcanics that are widespread southwest of Barstow, California (Schermer and Busby, 1994), and tend to be variably metamorphosed and sheared (Walker and others, 1990; Schermer and others, 1996; Pavlis and others, 1998).

Granitoid Rocks

Most of the granitoid rocks in the greater Fort Irwin area can be divided into two groups based on age and other characteristics. A third group that occurs locally south of Superior Lakes is Triassic in age (Miller and others, 1995) and will not be described further.

The older group is typically foliated and includes rocks of Jurassic and Early Cretaceous age. The Jurassic rocks are the most abundant, and are characterized by generally dark-colored outcrops and rugged mountainous exposures (map unit “mp” of Miller and others, 2014; blue in fig. 2). Jurassic rocks range in composition from diorite through quartz monzonite and monzodiorite to granodiorite and granite (Spencer, 1990a, 1990b; Yount and others, 1994; Miller and others, 1995; Schermer and others, 1996; Miller and Walker, 2002), and are 170–148 million years old (Ma) (Miller and Sutter, 1982; Schermer and others, 2001). Most of the Jurassic rocks are mafic with abundant hornblende and biotite, but volumetrically minor granite in this sequence is typically a white, felsic rock with less than 5 percent mafic minerals. An atypical granite of the Jurassic group is the Tiefort Granite, which underlies much of the Tiefort Mountains and ridges south of Tiefort Mountains (included in map unit “fp” of Miller and others, 2014; pink in fig. 2), and is felsic, medium to coarse grained, and contains minor biotite. The rocks of the Jurassic group are mineralized by epidote and chlorite in some places (Byers, 1960) and range from undeformed to mylonitic gneiss (Walker and others, 1990; Schermer and others, 1996; Schermer and others, 2001). Jurassic plutons of the area commonly host mafic dikes, including the Independence dike swarm of Late Jurassic age (Schermer and others, 1996). An approximately 105 Ma, syntectonic, myolinitic, biotite granite is exposed in the Tiefort Mountains area (Schermer and others, 2001; included in map unit “fp” of Miller and others, 2014; pink in fig. 2).

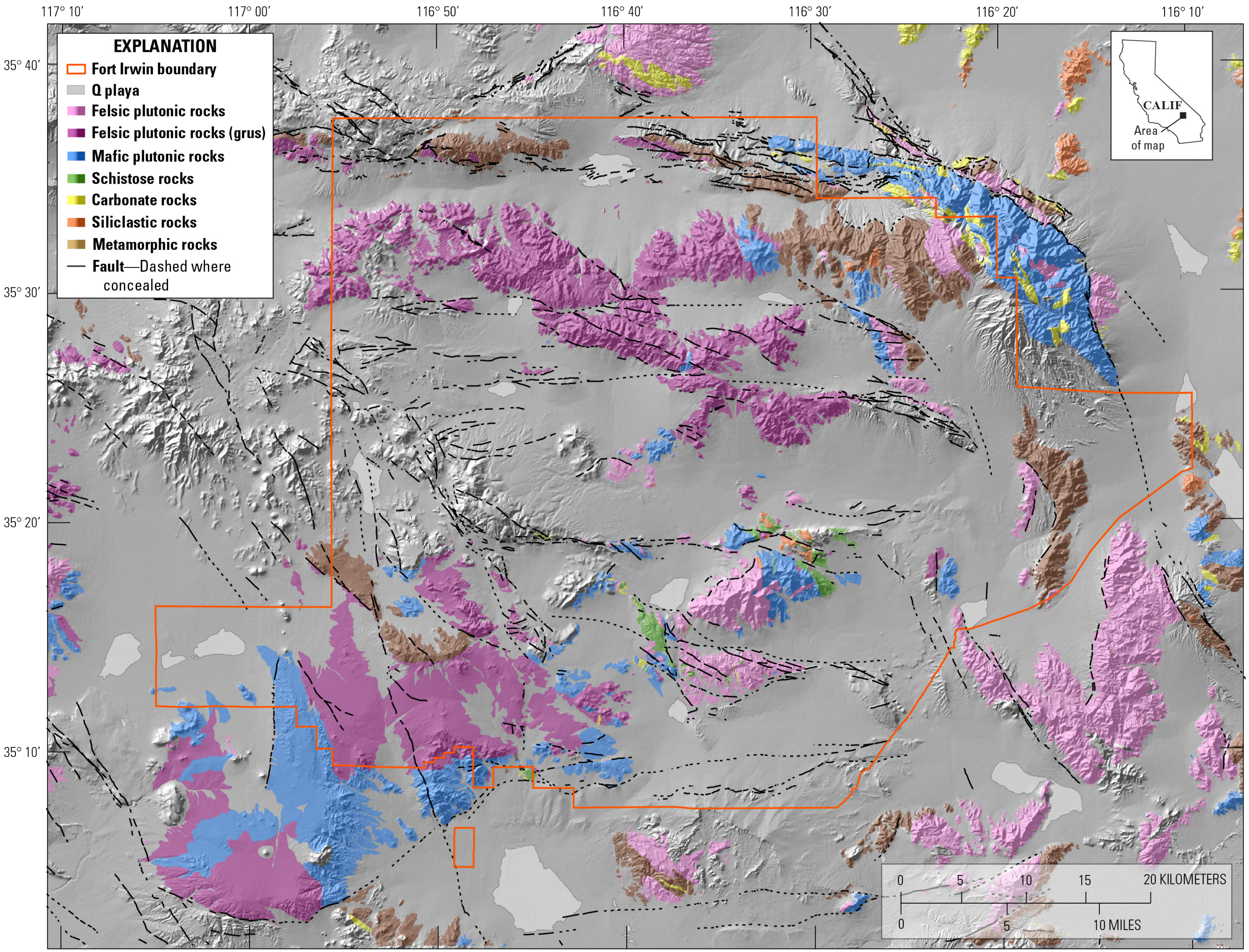

Figure 2. Map of the distribution of pre-Tertiary plutonic, metamorphic, and sedimentary rocks in the Fort Irwin area, California, displayed on a shaded-relief base map.

The younger, nonfoliated, granitoid group is Late Cretaceous (90–85 Ma), and is widespread in the Goldstone-Paradise Range area and much of the Granite Mountains (Miller and Sutter, 1982; Schermer and others, 1996; Schermer and others, 2001) (map unit “fp” of Miller and others, 2014; pink in fig. 2). Smaller plutons occur in several other mountain ranges, particularly north of the Garlock Fault. Cretaceous granitoids typically form pale-colored outcrops in mountains and pediments. Examples of pediments are found at Noble Dome of Byers (1960), west toward the Goldstone Mining District, and west of the Paradise Mountains. The granitoids typically are medium- to coarse-grained monzogranite and syenogranite and in many locations have sparse biotite as the mafic mineral. However, a large pluton that lies west of Noble Dome is distinctive in that muscovite is its main accessory mineral, and in places includes garnet as well (Yount and others, 1994; Schermer and others, 1996). The Cretaceous granitoids commonly weather to tors as a result of grain-by-grain disintegration (map unit “fpg” of Miller and others, 2014).

Miocene and Pliocene Volcanic and Sedimentary Rocks

Miocene volcanic rocks and sedimentary deposits occur (1) in a belt from west of Bicycle Lake to north of Goldstone Lake and beyond into the Eagle Crags volcanic field, (2) in a belt from eastern Alvord Mountain northeastward to the Avawatz Mountains, and (3) in the Quail and Owlshead Mountains and northeastward into southern Death Valley (Spencer, 1990a; Sabin and others, 1994; Schermer and others, 1996; Workman and others, 2002; Fridrich and Thompson, 2011; figs. 1 and 3). In the Fort Irwin area, these rocks can be divided into (1) early to middle Miocene (mostly 21–16 Ma) sequences that contain voluminous volcanic rocks and subordinate interbedded sedimentary rocks, and (2) middle to late Miocene (16 Ma to younger than 10 Ma) sedimentary sequences that include minor tuff beds (Spencer 1990b; Sabin and others, 1994; Schermer and others, 1996; Pavlis and others, 1998; Brady and Troxel, 1999; Miller and Yount, 2002; Fridrich and Thompson, 2011). In and west of Eagle Crags, andesite and rhyodacite flows and domes that are 15.2–12.4 Ma in age may represent a distinct volcanic field (Sabin and others, 1994). Distinctly younger volcanic rocks include a late Miocene (5.6 Ma) basalt that occurs from the Bitter Spring area northwest to Bicycle Lake, and is sandwiched between gravel deposits in many locations (Byers, 1960; Schermer and others, 1996). In the Black Mountain area southwest of the Superior Lakes, there is a Pliocene basalt field (~3.8 Ma age from Oskin and Iriondo, 2004). The Miocene and Pliocene volcanic and sedimentary rocks were deposited on the pre-Tertiary bedrock with prevolcanic paleotopographic relief as great as 100 meters [m] (Yount and others, 1994). Local topographic relief as great as 100 m was present in the volcanic field resulting from the development of cinder cones and lava flows (Yount and others, 1994). Miocene deposits therefore were unevenly distributed and the type of deposits, source area, paleotopographic controls, and subsequent structural dismemberment by faulting all must be considered.

Miocene Volcanic Sequence

Miocene volcanic rocks in the Fort Irwin area have been depicted in a variety of ways on various regional and local geologic maps (Byers, 1960; McCulloh, 1960; Jennings, 1994; Yount and others, 1994; Schermer and others, 1996; Walker and others, 2002; Workman and others, 2002; Luckow and others, 2005). The map of Miller and others (2014) divides volcanic rocks into mafic rocks (basalt to dacite with less than about 68 percent SiO_2 and represented with the map symbol “mv”) and felsic rocks (rhyodacite, rhyolite, and felsite with greater than about 68 percent SiO_2 and represented with the map symbol "fv"), and these rock units are represented in figure 3 as the blue "T mafic volcanic rocks" and pink "T felsic volcanic rocks", respectively. Most of the volcanism in the western part of Fort Irwin formed lava flows and tuffaceous sedimentary rocks along the eastern margin of the Eagle Crags volcanic field (Sabin and others 1994; fig. 3). In eastern Fort Irwin, the volcanic rocks are tuffaceous sedimentary rocks with a basaltic dike (plug) that intrudes granite (Sobieraj, 1994; Schermer and others, 1996). To the south in the Alvord Mountain area are thick deposits of mafic lava flows and tuffaceous rocks (Byers, 1960). To the north in the Quail Mountain and Owlshead Mountain areas is a series of predominantly mafic volcanic lava flows and tuffaceous sedimentary rocks (Wagner and Hsu, 1987; Luckow and others, 2005; Fridrich and Thompson, 2011).

The Eagle Crags area hosts the thickest, mostly felsic, volcanic accumulation that was erupted in two stages: 18.7–18.5 Ma and 15.2–12.4 Ma with ages determined by $^{40}Ar/^{39}Ar$ age spectrum plateau techniques on biotite, hornblende, or sanidine (Sabin, 1994; Sabin and others, 1994). Based on a thick volcanic section, numerous endogenous domes, numerous dikes (many of which are oriented radially to a common center), and a deep depression identified on gravity maps, Sabin and others (1994) proposed that the Eagle Crags volcanic field contains a trapdoor caldera hinged on the northeast. However, subsequent studies show that a large gravity low in the vicinity of the Eagle Crags volcanic field (Jachens and Langenheim, 2014) is not limited to the volcanic field, suggesting that the gravity low may represent variations in depth to basement and a thick pile of volcanic and sedimentary rocks with only minor caldera subsidence control.

Western Fort Irwin, including the Stone Ridge, Goldstone Mesa, Mars Hills, and Garry Owen areas and possibly the Dacite Dome to Southwest Ridge areas (fig. 1), exposes the eastern part of the Eagle Crags volcanic field and some slightly older tuffaceous deposits. The Miocene (21–16 Ma) volcanic sequence there was studied by Schermer and others (1996). The generalized sequence consists of:

- Dacite and rhyolite lava flows and pyroclastic deposits that are overlain by;
- Andesite to basaltic andesite lava flows and pyroclastic deposits; and
- Locally capped by olivine basalt lava flows (Schermer and others, 1996).

Although this sequence provides a generally sound geologic framework, there are more complicated sections in the Fort Irwin area, such as near Northwest and Coyote Ridges, where as many as five lava flows are interstratified with pyroclastic-sedimentary deposits (Schermer and others, 1996), and in the Goldstone Lake area where olivine basalt flows are interstratified with pyroclastic deposits in the dacite to andesite section. Based on the locally preserved vent facies and dikes that are consistent with conduits for the lava flows (Sabin and others, 1994; Schermer and others, 1996), the occurrence of endogenous domes (Sabin and others, 1994), and geometry of many of the dacite and rhyolite flows (including exogenous domes), the sequence of dacite, rhyolite, and basaltic andesite represents locally erupted material. In contrast, based on the composition and morphology of the olivine basalt flows in the Goldstone Mesa area, Schermer and others (1996) proposed that the olivine basalt had probably flowed from eruptive centers to the west or northwest.

To the south of Fort Irwin in the Alvord Mountain area, basalts and andesites of the Alvord Peak basalt of Byers (1960) are locally interstratified with arkosic sandstone and felsic pyroclastic deposits of the Clews and Spanish Canyon Formations (discussed in the "Miocene Sedimentary sequence" section). In addition, olivine basalt flows occur in the upper Spanish Canyon Formation and in the upper part of the lower member of the Barstow Formation (Byers, 1960). The thick accumulation of Alvord Peak basalt and andesite, locally exposed dikes, pipes,

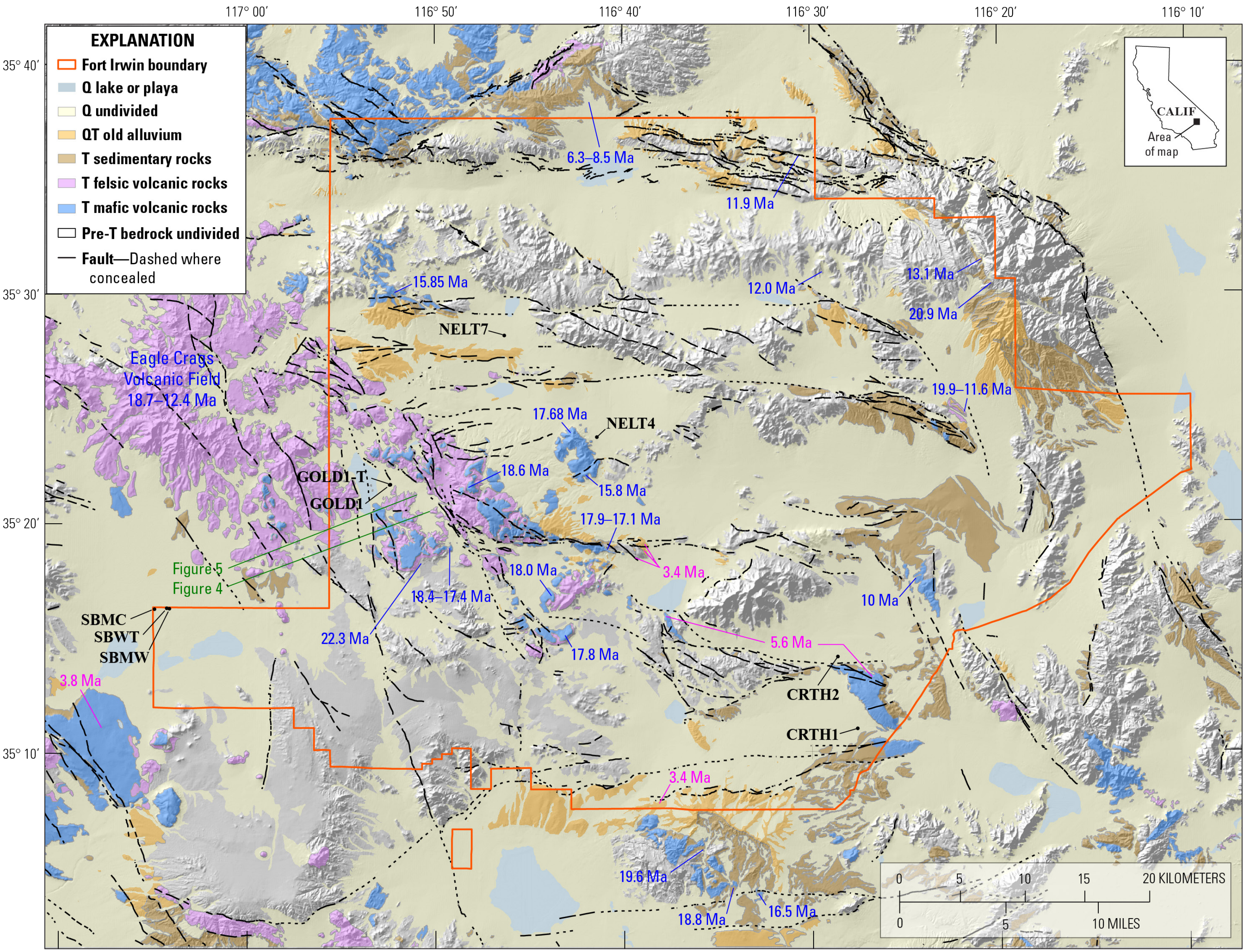

Figure 3. Map of the distributions of Cenozoic volcanic and sedimentary rocks and the early Pleistocene to Pliocene(?) extremely old alluvial fan deposits in the Fort Irwin area, California, displayed on a shaded-relief base map.

and small intrusive plugs of basalt and andesite that are compositionally the same as the lava flows, indicate that there were several vent areas within the Alvord Mountain area (Byers, 1960). In contrast, Byers (1960) proposed that the olivine basalt had probably flowed from eruptive centers to the west or northwest based on the composition and morphology of these flows.

North of the Garlock Fault Zone in the southwestern Owlshead Mountains is the southern section of another Miocene volcanic field that overlies a thin unit of arkosic sandstone deposited across Mesozoic plutonic rocks. This volcanic sequence has not been mapped in detail, but reconnaissance mapping and regional studies indicate a predominantly intermediate-composition suite of andesitic flows, breccias, and lahars with a minor component of more silicic (possibly dacitic or latitic) porphyritic crystal tuff (Wagner and Hsu, 1987; Fridrich and Thompson, 2011). At least some of the andesite flows appear to be hydrothermally altered with chlorite and (or) epidote. These rocks underlie or interfinger with more extensively studied sections of this volcanic field located to the north and northeast of the study area in the central and northern Owlshead and southern Panamint Mountains (Luckow and others, 2005). Volcanism in these areas produced a complex suite of extrusive rocks, including mixed lava flows and pyroclastic flows and fallout deposits that vary across a wide compositional range from felsic (rhyolites, dacites, rhyodacites) to more dominant intermediate and mafic compositions (andesites, basalts, trachybasalts). Extensive $^{40}Ar/^{39}Ar$ dating of these rocks indicates that volcanism in at least the central and northern part of the field was from 14 to 12 Ma (Luckow and others, 2005).

The map of the Fort Irwin area by Miller and others (2014) divides volcanic rocks into mafic rocks (basalt to dacite with less than about 68 percent SiO_2) and felsic rocks (rhyodacite, rhyolite, and felsite with greater than about 68 percent SiO_2); however, the types of deposits such as intrusions, lava flows, and tuffaceous (or pyroclastic) deposits are not separately identified. In some areas, a wide variety of rock types are represented by either unit. This chapter builds upon the classifications by Miller and others (2014), by refinement and clarification of the different rocks and divides volcanic rocks into:

1. Andesite (and related basaltic andesite) to rhyolite flows;
2. Tuffaceous deposits; and
3. Olivine basalt flows.

These three rock types have lithologic attributes that likely result in different hydrogeologic properties.

This threefold classification is based on maps by Byers (1960), Yount and others (1994), Schermer and others (1996), and Walker and others (2002), and ongoing mapping by D.M. Miller and D.C. Buesch. The three groups of rocks, however, are not represented consistently on these previously published maps, and improving a subdivision of volcanic rocks will be an important update to the geologic map of the Fort Irwin area.

Miocene Andesite to Rhyolite

Andesite to rhyolite occurs in the western part of Fort Irwin and into the Eagle Crags volcanic field, in the Alvord Mountain area to the south, the Avawatz Mountains to the east, and the Quail and Owlshead Mountains areas to the north (fig. 1; mostly the pink “T felsic volcanic rocks” in fig. 3). From the south-central area near Fort Irwin Garrison, andesite, dacite, and rhyolite lava flows occur in a swath of exposures northwest to the Garry Owen area and near Nelson Lake. South of Fort Irwin, exposures of andesite lava flows in the northern Alvord Mountain area are part of the Alvord Peak basalt of Byers (1960; described below in the “Miocene Basalt” section). East of Fort Irwin, volcanic rocks constitute a modest part of the

Miocene Avawatz and Military Canyon Formations in the southern, northern, and northwestern Avawatz Mountains (Spencer, 1990a, b; Brady and Troxel, 1999). As noted above, Miocene andesite with minor dacite or latite is extensively exposed in the southern Owlshead Mountains. In several of these areas, such as the western Fort Irwin and Alvord Mountain areas, andesite is interbedded with or compositionally includes andesitic basalt to basaltic andesite (Byers, 1960; Schermer and others, 1996). Some andesite, dacite, and rhyolite lava flows are associated with specific eruptive centers, and the compositionally different flows require detailed mapping to separate.

Although they differ compositionally, the andesite to rhyolite lava flows are grouped on the basis of:

1. Similar geometry of the deposits;
2. Crystallization;
3. Common autobrecciated fragments at the tops, bottoms, and lateral margins;
4. Flow banding; and
5. Abundant fractures that formed during cooling of the deposits.

Typically, the andesite to rhyolite flows form relatively thick and short (30–80 m thick and less than 1–3 km long) deposits resulting in moderate aspect ratios. Flows are typically crystallized, although some have vitric margins, and a few are dominantly glass. Domes of single or several overlapping flows have 100–300 m or more relief, and the radial distances of flow for domes is typically 600–1,200 m, resulting in small aspect ratios. These deposits typically have brecciated carapaces. For several of the flows and domes exposed in western Fort Irwin, these brecciated carapaces appear to be the source of avalanche or sedimentary breccia deposits. The correlations of sedimentary breccia to brecciated carapaces of the domes indicate that they were exogenous, in contrast to some of the endogenous domes described in the Eagle Crags volcanic field by Sabin and others (1994).

Many andesite to rhyolite flows and domes have extensive fractures that are interpreted as cooling fractures; however, some fractures formed from strain associated with faults, and some cooling fractures accommodated additional apertures or along-fracture separation as a result of structural deformation. Many cooling fractures are steeply dipping and can have long trace lengths, but neither orientation nor trace length is critical for identification as cooling fractures. Instead, small scale features such as the geometry of the fracture surface and the type of crystallization in the adjacent rock or mineralization along the fracture are the most diagnostic (Buesch and others, 1996; Buesch and others, 1999; Buesch, 2006).

Buesch and others (1996) adapted the joint profile and roughness coefficient (JRC) geometric fracture descriptors of Barton and Choubey (1977) to fractures in ignimbrites, and these descriptors can also be applied to lava flows. These descriptors include the “shape” of the fracture with terms that ranged from planar to very rough, and “surface roughness” with terms that ranged from smooth to very rough. Typically, early formed cooling fractures are planar to slightly planar or curviplanar and smooth to slightly smooth; and later-formed cooling fractures are slightly planar to slightly irregular and slightly smooth to slightly rough. Early fractures form when the rock is glassy and can develop thin rims (light gray with feldspar and (or) quartz, typically as spherulites) or thin borders (reddish purple with fine-grained feldspar and quartz) that penetrated from the fracture wall into the rock mass (Buesch, 2006). This crystallization of the wall rock results from the interaction of the vapor phase in the fractures within the glass. If the rock crystallizes before fractures form, the fractures will not have rims or borders (that is, there is no glass to react with) and are later formed fractures (Buesch, 2006). Fractures formed during cooling can have thin deposits of vapor-phase minerals such as tridymite or possibly opal, in addition to a wide range of minerals that form in minor amounts (Buesch and others, 1996; Buesch, 2006). Although fractures without rims, borders, or vapor-phase minerals can form during cooling (such as in isolated fractures), fractures without these features are described as indeterminate and could have formed at any time after the rock cooled back to ambient temperature (about 25 °C).

A good example of a rhyolite lava flow with several types of cooling fractures is exposed east of Goldstone Mesa (fig. 4). The main fractures are planar, smooth, and laterally continuous for various lengths, intersect at 90 to 120°, have rims 2 millimeters (mm) wide, and some have 1-mm wide borders. Cooling factures can also be slightly planar to curviplanar, slightly smooth, and have 1-mm wide rims. Many of the small, closely spaced fractures are slightly irregular, slightly rough, and have no rims. Although, the geometric relations of these small fractures to the larger cooling fractures are also consistent with formation during cooling; based on the shape, roughness, and lack of rims, they are classified as being "indeterminate" (meaning no petrologic evidence as to when they formed).

Identification of features such as geometry (shape and roughness) of fractures and the types of crystallization and mineralization adjacent to or along fractures can help distinguish fractures that formed during cooling from those formed during subsequent structural disruption. Identification of cooling fractures is important because (1) it constrains how and when the fractures formed, (2) the thermal expansion properties of a lava flow are inherent throughout the deposit, so fractures formed during cooling create a three-dimensional network that typically is highly connected, and (3) these cooling fracture networks are incorporated into the three-dimensional geometry of the lava flow, thus forming a reasonably predictable distribution of fracture permeability. In contrast, structurally induced fractures along faults or by deformation of structural blocks are localized and can be variable in orientation, spacing, and geometry along the fault or throughout the deformed block; therefore, there is uncertainty in the location and distribution of rock properties that can affect hydrogeologic properties. Although cooling and structurally induced fracture networks have neither been systematically documented nor hydrologically tested in the Fort Irwin area, these networks may have the potential to influence infiltration and lateral movement of groundwater.

Miocene Pyroclastic Rocks, Tuffaceous Sandstone, and Volcanic Avalanche Rocks

Thick pyroclastic rocks, tuffaceous sandstone, and avalanche deposits occur in the western part of Fort Irwin and into the Eagle Crags volcanic field, whereas thinner tuff-bed sections of sedimentary rocks occur in the Alvord Mountain area and to lesser extents in the Avawatz Mountains and northward into southern Death Valley. From the south-central area near Fort Irwin Garrison, sections of tuffaceous deposits occur in a swath of exposures northwest to Nelson Lake and the Garry Owen area. Many of these exposures are in close association with andesite to rhyolite described previously in the "Miocene Andesite to Rhyolite" section.

Tuffaceous deposits consist of primary pyroclastic flow and fallout tephra deposits, and secondary reworked tuff (tuffaceous sandstone) deposits in alluvial settings. These deposits consist of glass shards and pumice clasts, crystal fragments, and lithic clasts. Crystal fragments consist of sanidine and plagioclase along with hornblende and biotite, and some deposits have quartz. Most lithic clasts are aphyric to porphyritic volcanic rocks, and most are crystallized but some are vitric. Based on proximity of the tuffaceous deposits to explosive eruptive centers and the similarity in crystal compositions, many tuffaceous deposits are probably the products of explosive phases from these local eruptive domes and form proximal pyroclastic facies. Good examples occur at Goldstone Mesa, Pink Canyon, Stone Ridge, Pioneer Plateau, Garry Owen, and in borehole GOLD1 (figs. 1 and 3; Buesch, 2018). At the southern end of Goldstone Mesa, pumice clasts from a fallout tephra deposit near the base of the Miocene section have a $^{40}Ar/^{39}Ar$ hornblende total fusion date of 22.3 Ma (MacConnell and others, 1994). This age is slightly too old for the Eagle Crags volcanic field, so these deposits were probably derived from a different volcanic field. Some sections of tuffaceous deposits appear to be distal to the probable eruptive centers such as in the Nelson Lake area and eastern Fort Irwin areas, where they include primary pyroclastic flow and fallout tephra deposits that are finer grained than more proximal deposits. Typically, distal pyroclastic deposits are interbedded with reworked materials that formed in alluvial environments (described below in "Miocene Sedimentary Sequence" section). The pyroclastic and sedimentary facies form a complex network of sediment controlled by proximity to domes, redistribution by streams, and integration of those stream systems.

Based on thickness and lateral continuity of beds, variations in grain sizes and sorting, and the occurrence or absence of fractures, the tuffaceous deposits have moderately to highly variable lithologic (and possibly hydrologic) characteristics. Many tuffaceous deposits form individual beds that range in thickness from less than 1 centimeter [cm] to more than 5 m, with bedsets that are many meters thick, and composite sequences of pyroclastic deposits as thick as 20–80 m. Some pyroclastic flow deposits are partially welded, some of these are incipiently crystallized, and in these partially welded deposits, cooling fractures are common. Some tuffaceous beds are sufficiently indurated or partially cemented to maintain fractures, but most are not. As a result, many tuffaceous deposits do not have an integrated fracture network.

Sections of pyroclastic rock in the Goldstone Mesa, Pink Canyon, and Garry Owen areas contain interbedded monomictic breccia deposits that are 0.2 to 40 m thick and formed as avalanche deposits from partial collapse of domes. Most breccia fragments appear to be derived from a single flow in a rhyolite or dacite dome and the breccia tends to be poorly sorted, thick, and internally structureless. Some monomictic breccia deposits consist of bedsets of multiple breccia beds, each with a distinctive textural top and base, so the bedsets represent a series of collapses. A 40-m thick, monomictic breccia was penetrated in borehole GOLD1 (fig. 3), although this interpretation is based only on cuttings, an alternative interpretation is the deposit might be a fractured lava flow (Buesch, 2018). A similar monomictic breccia is exposed 2.2 km east-southeast of borehole GOLD1 along the northeastern part of Goldstone Mesa (figs. 3, 5). In surface exposures (fig. 5), the breccia forms a 4- to 5-m high cliff, contains blocks as large as 3 m in diameter to sand-sized grains, and fractures have trace lengths of 5 mm to greater than 5 m with apertures less than 1 mm to as much as 20 cm. The base of the avalanche deposit is locally exposed, where deformed (fluidized) substrate sandstone and conglomerate formed injection dikes into the breccia. Although the breccia is poorly exposed on many of the ridge tops in the area, the surfaces of the ridges are littered with blocks as large as 4 m in diameter that represent lag deposits. These relations indicate the monomictic breccia was deposited over an area of several square kilometers. The breccia has not been correlated to a specific source area; however, the closest exposed domes are 2–7 km from borehole GOLD1.

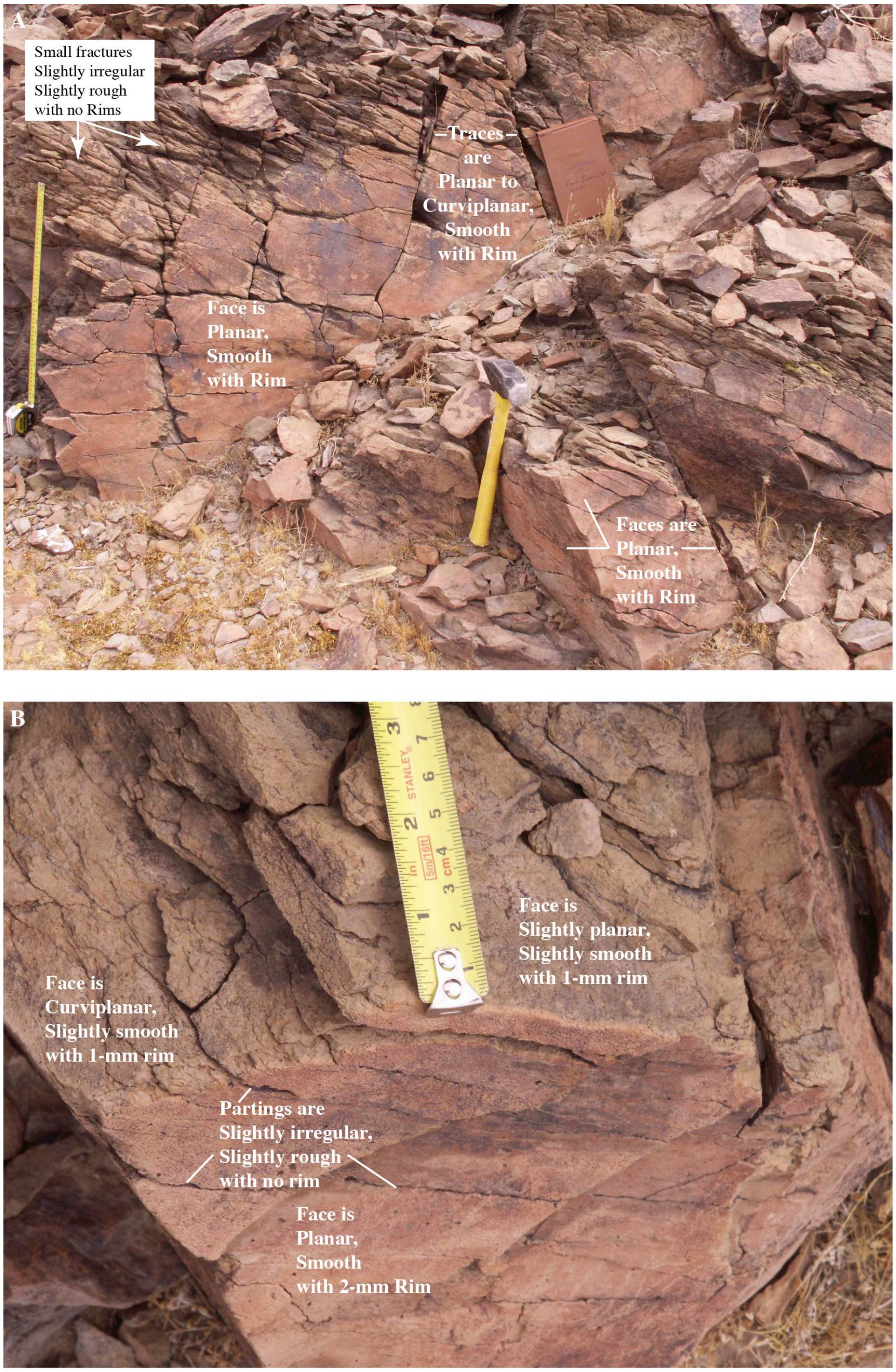

Figure 4. Photographs of fractures in a rhyolite lava flow formed during the cooling of the deposit in the Fort Irwin area, California, at lat 35°20.5' N, long 116°50.2' W (see fig. 3). *A*, Subhorizontal view of steeply to moderately dipping fractures. Tape is 50 centimeters. *B*, Close-up oblique view of top and front faces of fractures near hammer in *A*. Rims (light gray) and borders (reddish purple) are types of crystallization from the edge of a fracture into the rock (Buesch, 2006), and fracture shape (planar to irregular) and roughness (smooth to rough) are described in Buesch and others (1996).

Miocene Basalt

Miocene basalt flows occur in the western part of Fort Irwin, in the Eagle Crags volcanic field, in the Alvord Mountain area, locally north of the Red Pass area, and north of the Garlock Fault in the Quail and Owlshead Mountains (blue "T mafic volcanic rocks" in fig. 3). From the south-central area near Fort Irwin Garrison, basalt flows occur in a swath of exposures to the northwest including Stone Ridge, Goldstone Mesa, Pioneer Plateau, Mars Station, and into the Eagle Crags volcanic field and Garry Owens area. To the south of Fort Irwin, in the northern and central parts of the Alvord Mountain area, there are exposures of basalt in the Alvord Peak Basalt, and olivine basalt flows in the upper Spanish Canyon and lower Barstow Formations (Byers, 1960). North of the Red Pass area, basalts occur as north-trending intrusive rocks (Schermer and others, 1996). In the lower Wingate Wash and northern Owlshead Mountains areas, alkaline basalts (actually basanite and trachybasalt) are interstratified with trachyandesite flows, pyroclastic rocks, and sedimentary rocks (Luckow and others, 2005). In many of these areas, there are two types of basalts, those that tend to be sparsely porphyritic and geochemically basaltic andesite, (closely associated with andesites) and those that are porphyritic olivine basalts. However, these two types are not always identified separately.

Typically, the sparsely porphyritic basalt flows in the Coyote Ridge to Stone Ridge areas of Fort Irwin and in the Alvord Mountain area are closely associated with andesites. In the Coyote Ridge to Stone Ridge areas, andesitic basalt and basaltic andesite are interstratified, and along the southern edge of Stone Ridge, these flows form a section approximately 150 m thick. In the Alvord Mountain area, the Alvord Peak basalt consists of interstratified andesitic basalt and basaltic andesite, and in the central part of the exposed area are three or four lava flows with a total thickness of about 110 m. The flows are areally restricted. In both areas, the basalts are sparsely porphyritic with small (less than 0.5 mm) plagioclase and olivine phenocrysts, the andesites have similar minerals and textures, and the main distinction is the slight shift in anorthite content in plagioclase (that is, slightly greater or lesser than An_{50}). Thus, rocks are difficult to separate without petrographic or geochemical analysis, although there can be a few minor differences in fracturing and weathering characteristics.

Dikes of compositionally similar rocks, along with some localized vent structures, indicate that these sparsely porphyritic basalt flows probably erupted from local sources in the Alvord Mountain area and the Coyote Ridge or eastern Eagle Crags volcanic field areas (Byers, 1960; Schermer and others, 1996). For hydrogeologic purposes, these basalts share more characteristics with andesites than they do with the porphyritic olivine basalt flows.

Porphyritic olivine basalt flows in western Fort Irwin and Alvord Mountain areas typically form thin (0.5 to 3 m) deposits where individual flows can be traced for hundreds of meters; however, sequences of flows can range from 5 to 100 m thick (with a typical thickness of 25 m) and can be traced for more than 7 km. The length-to-thickness ratio of individual flows and sequences of flows is very high. Typically, plagioclase phenocrysts are less than 4 mm and olivine (and pyroxene) phenocrysts are less than 1 mm. Flows vary from vesicular to nonvesicular. As lava flows cooled and the rock contracted, numerous fractures formed and many have characteristic columnar joints. Many olivine basalt flows have a clinker of autobrecciated fragments at the top and (or) bottom of the flow. As a result of the cooling joints and possibly the porous clinker at the top and (or) bottom of the flows, a three-dimensional fracture network may exist throughout a basaltic rock mass.

Figure 5. Photographs of monomictic avalanche breccia exposed in ridges of the northeast Goldstone Mesa in the Fort Irwin area, California, lat 35°21.4’ N, long 116°51.1’ W (see fig. 3). *A,* Overview of field exposure with 35-centimeter long hammer. *B–E,* Progressively more detailed photographs of avalanche breccia; 10×135 millimeter pencil for scale.

In the Pink Canyon and Goldstone Mesa area of Fort Irwin where the porphyritic olivine basalts are most widely exposed, and in the Alvord Mountain area, there are no dikes or vents that might have erupted the olivine basalts. Both Byers (1960) and Schermer and others (1996) speculated that the flows might have come from vents somewhere northwest of the respective flow locations. Although there are no local sources (vent areas) for these olivine basalts, the flows are interstratified with locally erupted basalt to rhyolite flows, pyroclastic deposits, and sandstone deposits. For example, in the Pioneer Plateau and possibly borehole GOLD1 in the Goldstone Lake basin, olivine basalt flows are interstratified with dacite and rhyolite lava flows and pyroclastic rocks (David Buesch, 2011, ongoing mapping). Porphyritic olivine basalt flows interstratified with sedimentary sequences were penetrated in seven boreholes drilled from 2010–12 at Fort Irwin (Kjos and others, 2014; Buesch, 2018). In the boreholes, the basalt flows are as thin as 3 m (10 feet [ft]), but in four boreholes the basalt flows are at the bottom of the borehole and the minimum thicknesses are 12–29 m (40–95 ft). The basalt flows were penetrated at depths from 49 to 293 m (160 to 960 ft). In the Alvord Peak basalt, a scoriaceous, porphyritic olivine basalt flow interstratified with the thick basalt and andesite flows has been traced for a few kilometers (David Miller, 2011, ongoing mapping). Locally, in the middle of the Barstow Formation in the eastern Alvord Mountain area, there are three porphyritic olivine basalt flow units, the lowest of which has a $^{40}Ar/^{39}Ar$ date of 16.47 Ma (Woodburne and Reynolds, 2010). The importance of these potentially distant sources is that (1) eruptions from one volcanic field (or vent area) can be interbedded with lava flows and other deposits from a local field, and (2) there is a good possibility that these far-traveled flows are buried in what are now intervening valleys.

Miocene Sedimentary Sequence

Exposures of Miocene sedimentary rocks occur (1) locally in the western Fort Irwin area, (2) mostly in a belt in the eastern Fort Irwin area that passes from the Alvord Mountain area northeast to the Avawatz Mountains, and (3) in the Quail and Owlshead Mountains and northward into southern Death Valley (Grose, 1959; Byers, 1960, Brady, 1984, 1986a, b; Spencer, 1990a; Fillmore, 1993; Sobieraj, 1994; Schermer and others, 1996; Brady and Troxel, 1999; Fridrich and Thompson, 2011; brown “T sedimentary rocks” in fig. 3). In the Fort Irwin area, these sedimentary rocks are shallowly to moderately dipping, medial to distal alluvial fan and fluvial deposits of early and middle Miocene age, and include lesser lacustrine strata (Byers, 1960; Sobieraj, 1994; Schermer and others, 1996; Pavlis and others, 1998). Along the eastern margin of the Fort Irwin area, older deposits of the Avawatz Formation are mainly coarse conglomerate, including landslide breccia in places. The older (early to middle Miocene) deposits in the eastern Alvord Mountain area include the Clews Formation that is primarily coarse conglomerate and sandstone with minor tuffaceous deposits. There is locally derived volcaniclastic conglomerate within the Alvord Peak basalt (Byers, 1960; Fillmore, 1993; David Buesch, 2012, ongoing mapping). Both rock units are overlain by the Spanish Canyon Formation that consists primarily of tuffaceous deposits interstratified with sandstone and minor coarse conglomerate capped by olivine basalt flows (Byers, 1960). The Spanish Canyon Formation includes a tuff from the base of the type section that is 19.6±0.2 Ma using zircon U-Pb dating techniques and the Peach Spring Tuff (18.78±0.02 Ma in Ferguson and others, 2013) in the middle of the formation (Buesch, 2012; Buesch and others, 2013). In the northern, eastern, and southeastern Alvord Mountain area, the Spanish Canyon Formation is overlain by the early to middle Miocene Barstow Formation (Byers, 1960), that consists of alluvial and lacustrine deposits of interfingering arkosic and locally volcaniclastic, siltstone, sandstone, and cobble conglomerate, along with rhyolite tuff. Similar sequences are poorly exposed northeast from Alvord Mountain to east of Tiefort Mountain and near the east end of the Fort Irwin Fault on the eastern part of an area informally referred to as the Central Corridor Basin (Sobieraj, 1994; Schermer and others, 1996; Pavlis and others, 1998; fig. 1). Fallout tephra deposits in the eastern part of the Central Corridor Basin (fig. 1) have $^{40}Ar/^{39}Ar$ ages of 19.0 Ma for a lapilli tuff near the base of the sedimentary section and 11.65 Ma for a crystal-rich tuff in the lower part of the sedimentary section located in a somewhat structurally and stratigraphically complex exposure (Soberaj, 1994; Schermer and others, 1996; fig. 3). An ash bed in the upper part of the sedimentary section located east of Tiefort Mountain has a tephrochronologic age of 10 Ma (Miller and Yount, 2002). Also in the areas east of Tiefort Mountain (south and east of the Tiefort Mountain Fault; fig. 1), megabreccia deposits interpreted as landslide deposits overlie ~10 Ma (Miller and Yount, 2002) fluvial and lacustrine deposits (Schermer and others, 1996; David Miller, 1995, and ongoing mapping).

Sedimentary rocks exposed in the “Crash Hill” area near Nelson Lake in western Fort Irwin are presumed to be Miocene in age based on the abundance of volcanic and tuffaceous material in part of the section. The rocks at Crash Hill are similar to subsurface rocks in the basin concealed by the Quaternary deposits. There are three main lithostratigraphic units. The lowest (prevolcanic) unit consists of arkosic sandstone and conglomerate, the upper part of which contains a few thin rhyolite tuff beds that were probably deposited in medial, moderate-gradient alluvial fan environments. The middle (synvolcanic) unit consists of lithic and (or) tuffaceous sandstone and siltstone (mostly with tuffaceous matrix or redeposited tuffaceous grains) interbedded with minor cobble conglomerate and numerous pyroclastic (mostly fallout tephra) deposits that were probably deposited in distal, shallow-gradient alluvial fan to fluvial, and possibly lacustrine environments. Samples from a 13-cm thick, crystal-poor, vitric fallout tephra deposit have potential tephrochronologic correlations to a ~6 Ma tephra from Fish Lake Valley, or to a 12–10 Ma tuff from the southern Nevada Volcanic Field (Elmira Wan, USGS, written commun., 2014). The upper (postvolcanic) unit in the Crash Hill area consists of sandstone and conglomerate (mostly pebble and some cobble), and the lower part contains a few fallout tephra beds. Overall, there is an increase in grain size and bed thickness in these postvolcanic rocks compared to the synvolcanic rocks. The postvolcanic sandstone and conglomerate were probably deposited in medial to distal, moderate to shallow gradient, alluvial fan environments. Because of uncertain palinspastic restoration along left-lateral strike-slip faults, and the presence of a potential paleotopographic ridge of plutonic rocks along the east side of the Nelson Lake basin, it is not known how this section of rocks exposed at Crash Hill correlates to the section of alluvial fan and lacustrine deposits in eastern Fort Irwin that were described by Sobieraj (1994) and Schermer and others (1996).

Six of the seven NELT-series boreholes in the Nelson Lake basin bottomed in the inferred Miocene section, mostly at depths of 203–276 m (Kjos and others, 2014; Buesch, 2018). Only borehole NELT4 (fig. 3) penetrated the bottom of the inferred Miocene section into metamorphic (gneissic) rocks at 256 m (Buesch, 2018). Typically, the boreholes penetrated 21–40 m of inferred Quaternary to Pliocene age deposits and 170–250 m of inferred Miocene age sedimentary rocks (Buesch, 2018). Based on the types and sizes of cuttings fragments and a limited number of pieces of core, the inferred Miocene section consists of sandstone interbedded with pebble and cobble conglomerate, with local siltstone and possibly primary pyroclastic deposits (Buesch, 2018). These sedimentary rocks were likely deposited in alluvial fan, fluvial, and lacustrine environments, and source areas probably were in volcanic highlands to the west and southwest. Borehole NELT7, in the northern part of the basin (fig. 3), has sandstone and conglomerate that were probably derived from the pre-Tertiary granitic rocks north of the basin; however, the matrix appears to have a significant tuffaceous component that was probably derived from fallout tephra deposited on the highlands or mixing of tuffaceous sediments derived from highlands to the west. The thick section of presumed Miocene alluvial or fluvial sandstone and conglomerate in the Nelson Lake basin is consistent with the apparently deep basin modeled by gravity studies (Jachens and Langenheim, 2014, their fig. 5).

In the Goldstone Lake basin, rocks inferred to be of Miocene age were encountered in borehole GOLD1 (fig. 3). Most of the sedimentary rocks have a tuffaceous component in the sand-sized and finer grained matrix. In contrast to the Nelson Lake basin, there are several nonwelded to partially welded ignimbrites (Buesch, 2018).

Miocene sedimentary rocks are also exposed discontinuously within and north of the Garlock Fault Zone in ranges that form the southern and western margins of southern Death Valley (brown “T sedimentary rocks” in fig. 3). One of the main sedimentary units is the middle to upper Miocene Military Canyon Formation exposed in the northern, northwestern (Noble Hills), and western Avawatz Mountains and locally in the adjoining upper piedmont between the northwestern Avawatz and southeastern Owlshead Mountains (Brady, 1984, 1986a, 1986b; Brady and Troxel, 1999). This formation contains a generally fining-upward sequence consisting of: (1) a lower member of cobble-boulder conglomerate; (2) a middle member of conglomerate grading upward into sandstone and mudstone, with some interbedded flows of hornblende andesite dated at 14–11 Ma; and (3) an upper member variably composed of sandstone, mudstone, limestone, gypsum, chert, and halite that in places contain interbedded fallout ash beds dated at 9–6 Ma. These deposits probably formed in a narrow, elongate, mostly closed basin within the proto-Garlock Fault Zone that has subsequently been structurally dismembered and internally folded within a series of faultblocks bounded by internal strands of the eastern Garlock Fault Zone, the Southern Death Valley Fault Zone, and thrust faults in the northeastern Avawatz Mountain. An additional, less well studied sedimentary sequence of primarily coarse-grained conglomerate and sedimentary breccia was deposited unconformably on pre-Tertiary rocks and (or) middle Miocene volcanic rocks along the southern margin of the Owlshead Mountains (Fridrich and Thompson, 2011). There is no published work on the precise stratigraphy, depositional framework, and age of these sedimentary sequences, but they most likely represent deposition in one or more successor basins that are approximately correlative with the middle to upper Military Canyon Formation.

Facies and Architecture of the Volcanic Field and Surrounding Region

Rocks deposited during the Miocene, especially south of the Garlock Fault, consist of:

1. Prevolcanic sandstone and conglomerate deposited in alluvial and possibly fluvial environments,
2. Lava flows and pyroclastic rocks deposited in constructional volcanic fields that developed on exposed bedrock or prograded across peripheral alluvial and fluvial environments,
3. Sandstone, conglomerate, and locally siltstone deposited in alluvial, fluvial, and locally lacustrine environments that were outside of, but contemporaneous with, the active volcanic fields, and
4. Postvolcanic sandstone and conglomerate deposited in alluvial and possibly fluvial environments, and locally lacustrine environments.

Locally, megabreccia deposits resulted from landslides and rock avalanches. Details on the descriptions and interpretations of the clast types and provenance, sedimentary facies, and paleoflow direction indicators have been presented previously by Byers (1960), Brady (1984, 1986a, b), Spencer (1990a), Fillmore (1993), Sobieraj (1994), Schermer and others (1996), Pavlis and others (1998), Brady and Troxel (1999), Luckow and others (2005), and Fridrich and Thompson (2011).

Prevolcanic sandstone and conglomerate were derived from local pre-Tertiary bedrock and were deposited in alluvial and fluvial environments. Examples of these rocks in Fort Irwin include exposures in the lower part of the Crash Hill section in the west, the lower part of the eastern Central Corridor Basin section, the Clews Formation in the Alvord Mountain area, and the lower Avawatz and Military Formations in the Avawatz and southern Owlshead Mountains. Additionally, the Avawatz and Clews Formations include megabreccia deposits that indicate local areas of high topographic relief. Based on clast types and provenance, sedimentary facies, and paleoflow direction indicators, all of these areas were probably separate basins, locally bounded by areas of high relief. The Avawatz and Military Formations in Avawatz and southern Owlshead Mountains were derived from areas to the east and southeast.

Volcanic and synvolcanic deposits associated with Eagle Crags volcanic field (as far east as the Dacite Dome) consist of andesite to rhyolite lava flows as proximal eruption facies, and pyroclastic flow and fallout tephra deposits that were proximal to distal facies relative to eruption sites. Reworked clasts derived from these deposits were deposited as tuffaceous sandstone in medial to distal alluvial fan to fluvial environments. Lava flows, especially domes, formed areas of large relief surrounded by onlap and buttress unconformities with pyroclastic and redeposited sediments. As the volcanic field developed, all the facies resulted in the growth of a constructional architecture representing the complex accumulation of migrating eruption sites and deposition between and beyond these local topographic highlands. Because basaltic lava flows can have long flow paths, these flows could have erupted elsewhere and been interstratified with the local facies in many parts of the section.

The volcanic and synvolcanic sedimentary rocks in Alvord Mountain area underwent similar processes of the growth of a volcanic field as did the Eagle Crags volcanic field, and resulted in the accumulation of the Alvord Peak basalt, the Spanish Canyon Formation, and lower part of the Barstow Formation. The restricted compositional range, small areal extent, and small volume of the Alvord Peak basalt indicate the lava field probably was active for a relatively short period of time. The pyroclastic and tuffaceous rocks in the Spanish Canyon Formation and lower two-thirds of the Barstow Formation (and minor amounts of tuff beds in the Clews Formation) represent pyroclastic material transported into the area where they interacted with arkosic and locally volcaniclastic sediments in alluvial fan, fluvial, and locally lacustrine environments to form interstratified deposits. Again, because basaltic lava flows can have long flow paths, these flows can erupt elsewhere and be interstratified with the local facies in many parts of the section.

Synvolcanic equivalent sections in the eastern Fort Irwin and the Avawatz and southern Owlshead Mountains typically are sandstone and conglomerate deposited in alluvial to fluvial environments. Identification of these sections as synvolcanic is based on locally interstratified ash and tuffaceous deposits. Based on the minimal pyroclastic component to these sections, the sections probably represent different depositional basins than those in western Fort Irwin and Alvord Mountain areas. In the northern Owlshead Mountains, there is a complex interstratification of lava flows, pyroclastic rocks, and re-deposited volcaniclastic rocks.

Postvolcanic epiclastic sandstone and conglomerate in western and eastern Fort Irwin, eastern Alvord Mountain, and the Avawatz and Owlshead Mountains were deposited in alluvial fan, fluvial, and locally lacustrine environments with interstratified megabreccia in eastern Fort Irwin and the Avawatz and Owlshead Mountains. Typically, there is an upward fining of grain size in many of these sections. Based on clast types, sedimentary facies, and paleoflow direction indicators, these areas were probably separate basins during the middle to late(?) Miocene.

Contacts or transitions from the Miocene postvolcanic sandstone and conglomerate to overlying Pliocene and Quaternary deposits are locally exposed, but in several areas the contact has not been identified. In western Fort Irwin, there are few exposures of what might be the upper Miocene section, and significant angular unconformities have not been identified; therefore, it is possible that some of the uppermost sediments (mapped as the unit QToa by Miller and others, 2014; light brown "QT old alluvium" in fig. 3) might be late Miocene in age. In the Alvord Mountain area, the contact of Barstow Formation with the overlying Goldstone gravel is locally gradational or a slight angular unconformity (Byers, 1960; Wyatt, 2005; Miller and others, 2011). The Goldstone gravel includes long-traveled clasts from the Goldstone area in western Fort Irwin and represents regional integration of an east to southeast flowing drainage system (Miller and others, 2011).

Latest Miocene and (or) Pliocene Basalts

Two basalt flows in the Fort Irwin area appear to be significantly younger than other basalts based on geochronologic studies. The older of the two is a series of basalt flows that are discontinuously exposed from (1) an area in southeastern Fort Irwin near Bitter Springs and along a ridge informally known as the "The Whale" to (2) an exposure southeast of Bicycle Lake to (3) small exposures at Coyote Ridge (fig. 1; blue "T mafic volcanic rocks" in fig. 3). These basalt flows are collectively (and informally) referred to as the Bicycle Lake basalt (Miller and others, 2001). The basaltic lava flows have a late Miocene age of 5.6±0.2 Ma (Schermer and others, 1996), and this age was cited by Miller and Yount (2002); however, they also reported a younger and less precise age of 3.4 Ma for an exposure in the Coyote Canyon area. Compositionally, the rock is andesitic basalt that is very vesicular to nonvesicular with rare olivine and possibly hypersthene microphenocrysts in a very fine-grained groundmass (Byers, 1960; Yount and others, 1994). Discontinuous exposures of the basalt flows result from (1) burial by younger sedimentary deposits, and (2) structural disruption and isolation of structural blocks along the Coyote Canyon and Bicycle Lake Faults that have accommodated an estimated 4.7 km of left-lateral strike-slip separation (Schermer and others, 1996).

Pliocene Black Mountains basalt caps the Barstow Formation in the Gravel Hills (Oskin and Iriondo, 2004; fig. 1; blue "T mafic volcanic rocks" in fig. 3). The Black Mountains basalt is typically fine grained and vesicular, has diabase groundmass texture, and is highly fractured with some hexagonal but mostly irregular jointing (Dibblee and Minch, 2008). In the northern Black Mountains, the basalt consists of five lava flows that are described mostly in terms of lava flow morphology to determine separation on the Blackwater Fault (Oskin and Iriondo, 2004). The two uppermost flows (flows 4 and 5) have large (1–3 mm) olivine phenocrysts, and flow 4 has distinctive quartz monzonite xenoliths (Oskin and Iriondo, 2004). The $^{40}Ar/^{39}Ar$ ages of lava flows 2, 4, and 5 are 3.77±0.11 Ma, 3.74±0.05 Ma, and 3.56±0.08 Ma, respectively (Oskin and Iriondo, 2004). The stratigraphically sequential ages are consistent with development of the field in about 210,000 years. These three ages have a weighted mean of 3.70±0.01 Ma within a 2-sigma error.

Unconsolidated Deposits

Unconsolidated deposits range in age from Pliocene to recent, and commonly underlie the topographic basins of the Fort Irwin area. Over most of the training center, alluvial fan deposits grade from coarse-grained proximal deposits in and near mountain fronts to fine-grained distal deposits near basin axes, where they merge in many cases into playa lake deposits. Most of these alluvial fan and playa deposits range in age from modern (active) to middle Pleistocene (Yount and others, 1994). In a few places, older unconsolidated deposits have been deformed along faults; there, alluvial fan deposits extend high onto mountain flanks or are perched on ridges, such as areas of Coyote Ridge northwest of Bicycle Lake and the north flank of Alvord Mountain. These older deposits have been dated as Pliocene and early Pleistocene (Miller and Yount, 2002; Miller and others, 2011).

Pliocene(?) and Early Pleistocene Deposits

Most of the older unconsolidated deposits in the main section of Fort Irwin south of the Garlock Fault Zone are exposed in a belt of low hills along the Coyote Lake Fault (north of Coyote Lake), near Langford Well Lake, and along the north flank of Alvord Mountain (Byers, 1960; Miller and others, 2014; light brown “QT old alluvium” in fig. 3). These distinctive fluvial gravels are composed mainly of granitic debris, and consist of bedded gravelly sand. Transport indicators, such as crossbedding, suggest eastward flow of streams, as do the distinctive clasts in the deposit that were derived from the Goldstone area (Byers, 1960). Clasts that indicate this provenance include colorful striped metamorphic rocks, white muscovite-bearing granite, and less commonly, granite with muscovite and garnet (Miller and Yount, 2002). A Pliocene ash bed in the deposit has been dated at about 3.4 Ma (Miller and Yount, 2002). The same ash is present in a wetland deposit northwest of Bicycle Lake and interfingers westward with alluvial gravel of local provenance (Miller and Yount, 2002). The gravel unit, informally termed the Goldstone gravel by Miller and others (2011), is about 300 m thick, and becomes finer grained eastward; it evidently marks uplift and persistent stream flow from the Goldstone area.

Exposures of Pliocene and early Pleistocene gravels (light brown “QT old alluvium” in fig. 3) occur in the western part of the Nelson Lake basin, the northern side of Coyote Ridge, and northeastern Fort Irwin west of the Avawatz Mountains. In these locations, locally derived clasts in the gravel indicate that mountain sources and valley sinks were similar, in general, to those that exist today. In detail, modern streams near these deposits carry somewhat different bedload, indicating that sediment sources have changed.

Although outcrops of Pliocene and early Pleistocene gravels are sparse in much of Fort Irwin south of the eastern Garlock Fault Zone, such deposits are plausibly in the subsurface, and probably have been encountered in boreholes. As with the Goldstone gravel, these deposits are generally coarse in the west and fine eastward. The principal argument comes from study of deposits farther south of Fort Irwin. Pliocene and early Pleistocene deposits extend in a belt from the Calico Mountains eastward to south of Alvord Mountain (Miller and others, 2011). Like the Goldstone gravel, these deposits (the Yermo gravel) share a unique source area and exhibit eastward-fining of grain size. Both the Goldstone and Yermo gravels define east-trending paleovalleys that are aligned with, and are found along the north side of, Quaternary/Holocene? faults, the Coyote Lake Fault and the Manix Fault, respectively. This relation suggests that the east-striking faults here formed spatially coincident valleys that drained rivers sourced farther west. Similar east-trending valleys that originate in high ground on the west can be found in Fort Irwin, suggesting that similar paleogeography may have existed there. Inferred Pliocene and early Pleistocene deposits at depth in Nelson Lake basin and north of Tiefort Mountains may coarsen westward and be composed of Miocene volcanic rocks that underlie the western highlands (Buesch, 2018).

Pliocene and early Pleistocene deposits do occur in highland areas north of the Garlock Fault Zone within the northern, northwestern, and western Avawatz Mountains and along the southern margin of the Owlshead Mountains (Brady, 1986a, b; Fridrich and Thompson, 2011). These sediments are composed mostly of variably bedded, weakly to unconsolidated gravel beds that occur in highly dissected, distinctive ridges with no preservation of original depositional surfaces and no clear relations to modern depositional systems. Typically, these units unconformably overlie with angular discordance more highly deformed pre-Tertiary rocks and (or) middle to upper Miocene volcanic or sedimentary rocks (described above in the "Pre-Tertiary Rocks" and "Miocene and Pliocene Volcanic and Sedimentary Rocks" sections), and these unconformity relations occur within or along the flanks of highland areas. These relations suggest syn to postdepositional uplift, typically with only moderate internal structural disruption other than broad arching, along bounding strike-slip or thrust-fault systems on the frontal escarpments of these ranges. Several pronounced ridges underlain by gravel deposits of this unit also occur within actively forming, doubly plunging anticlines in the upper piedmont embayment areas between the northwest Avawatz and southeastern Owlshead Mountains. There are relatively few reported exposures of finer grained medial- to distal-fan facies of these gravel deposits, but presumably these units may occur in the subsurface beneath piedmont Quaternary deposits in the adjoining basins. There is no direct age control for these gravelly deposits in the map area, but several 3.5–0.7 Ma fallout ashes have been identified in probably correlative fine-grained basin-interior facies of this unit along the Southern Death Valley Fault Zone in southern Death Valley just north of the map boundary (Green, 2009).

Quaternary Deposits

Quaternary deposits (light yellow "Q undivided" in fig. 3) are most readily understood by examining their landforms and internal characteristics, so geomorphology is a powerful tool for describing the deposits. The geomorphology of the Fort Irwin area is typical of many parts of the Mojave Desert, consisting of rugged mountains separated by broad valleys that are generally alluvial fan piedmonts that grade into playas at terminal drainage points. The physical substrate elements of the landscape affect its surficial geology, and by studying the processes that have moved sediment over time, predictions can be made of the physical properties of surface materials. Surficial geology also provides information on surface hydrology that not only leads to predictions of phenomena such as flooding, but also is essential for predicting available water for vegetation and deep infiltration to recharge basins.

The Fort Irwin area contains basins that at the surface are composed primarily of unconsolidated loose sediment. They, like the mountains that bound them, generally trend east-west. Many basins are internally drained and contain a playa at their lowest points, but others are integrated and drain externally, such as the several that drain to the Bitter Springs area, itself a source area for drainage to the Cronese Lakes (fig. 1). Overall altitudes of valley bottoms and mountain tops generally increase from southwest to northeast, from a low of 520 m at Coyote Lake to a high of 1,875 m in the Avawatz Mountains.

Arid land geomorphic processes that form sedimentary deposits include both transportation and depositional processes; erosional processes further modify the deposits and landscape. These transportation and deposition processes can be grouped as fundamentally (1) eolian (wind transport), (2) fluvial and alluvial (water transport), and (3) gravity-driven (topple, slide, creep, and slump of material on mostly steep slopes). Each of these transportation and deposition processes has unique characteristics in terms of the physical properties of the ensuing deposit as well as the morphology of the surface of the deposit. This report primarily describes deposits formed by fluvial processes. Eolian sand dunes are mainly located near Superior Lakes and Langford Well Lake in Fort Irwin, and more extensive dune fields lie outside of the installation. Lacustrine deposits are also mapped around Superior Lakes.

Processes that act on these deposits include erosion, weathering, and pedogenic soil development; of these, pedogenic soil development is the most important. Pedogenesis includes effects of chemical and physical modification of minerals from weathering as well as deposition and translocation of dust, solutes, and minerals through the deposit by water percolating down from the surface and by biota transport. Soil development commences when the surface of the new deposit is stable; that is, when it is no longer receiving sediment or being eroded. As a result, soil development is progressive and can be described in a sequence of stages that is roughly related to the age of the deposit (Harden and Taylor, 1983). Yount and others (1994) described the evolution of soils and surface morphology of deposits in southwestern Fort Irwin, correlating to the chronosequence of Reheis and others (1989) near Silver Lake to infer approximate ages for deposits and soils in the Fort Irwin area.

Types of Deposits

Alluvial fans and piedmonts (or bajadas) are landforms produced by deposition and transportation systems flanking mountains that route sediment eroded from the mountains toward valley axes. Slope generally decreases toward the valley (from proximal to distal fan) with an attendant overall decrease in rock clast sizes and decrease in degree of incision (channeling). Two results of the changes in clast size and degree of incision from proximal to distal fan include decreases in bulk permeability and increases in vegetation cover because of more widely distributed water in shallower channels. Proximal fans more commonly have deposits formed from debris flows and concentrated flood deposits with attendant very large clast sizes and large channels and levees. Distal fans, by contrast, chiefly have deposits formed by poorly channelized or sheet flow processes with attendant relatively thin moderately size-sorted beds of fine gravel and sand.

Piedmonts formed chiefly from grus-producing granite form a special class of alluvial fans. Because clast size is controlled by the grus weathered from rock, fine gravel and sand are present throughout grussy piedmonts. The relatively small and consistent clast size results in broad, gently undulating piedmonts that exhibit little channel incision.

Valley-axis streams collect surface discharge into through-going drainages that lie transverse to streams on fans. They differ from piedmonts in that they consist mainly of small clasts that have mixed sources from many mountains and piedmonts. The better size sorting and concentration of river flow for sustained periods in axial valleys contributes to an abundance of regularly and thinly bedded gravelly sand as the main deposit. Valley-axis washes commonly occur both as broad braided streams and as incised narrow channels; these forms may alternate along a single wash. Overbank “floodplain” deposits are common along big wash systems; these layers of muds contribute to generally lower permeability of valley-axis stream deposits as compared to piedmont deposits. Another feature of valley-axis systems is complexes of fringing eolian sand dunes and sheets because the big streams are a major provider of newly deposited sand that is readily available for wind transport and deposition on adjacent parts of the basin.

Axial streams typically receive more sustained flow than channels on fans, and as a result are probably the main sites of modern deep recharge.

Playas and playa margins form distinctive geomorphic environments in basin interiors by virtue of their flatness and consequent very fine clast sizes. Playas of the Fort Irwin area are the termini for valley-axis stream and piedmont surface discharge within a basin or local system of linked drainages, but elsewhere in the Mojave Desert playas also form at flat spots in through-going wash systems (such as Silurian Lake). The flat setting leads to deposition of both fine bed load and suspended load, resulting in typical fine sand, silt, and clay composition for playa deposits. This composition leads to low bulk permeability, shrink-swell behavior (commonly manifested as polygonal desiccation cracks), and (along with alkalinity in some cases) a lack of vegetation. Near margins of playas, grain flows may be interbedded with finer materials and lead to greater permeability; these areas commonly have sparse vegetation. Playa sediments of the Fort Irwin area are typically brown to red, vaguely bedded, and poorly sorted.

Playas are commonly ringed by marginal zones of complex deposits formed from several processes: (1) inundation by periodic shallow lakes forms shoreline deposits such as beach ridges and sand sheets (especially prevalent at Superior Lakes); (2) distal alluvial fan wedges form from sheetflow; and (3) deposition of eolian mud and sand eroded from the playa bed creates dunes and sheets. These deposits are both vertically stacked and laterally mingled to form a complex zone. As a result, the playa margin environment is complex in terms of its sediment properties, landforms, and vegetation; it may be an environment extremely sensitive to changes in a variety of processes, such as surface runoff and rainfall, wind events, and changes in temperature. During periods of sustained stream flow, such as during glacial epochs, some playa-floored basins of Fort Irwin may have supported perennial lakes. As a result, deposits at depth may include well-sorted green or gray fine sediments of lacustrine origin.

Groundwater discharge deposits, such as those formed at springs, wetlands, and riparian corridors are generally vegetated by grasses, rushes, sedges, and other phreatophytes. They form loose, white to pale brown, puffy and crusty deposits of silt, clay, and fine sand that may have salt crusts. Areas of active discharge may have open water as pools or streams, but generally do not in Fort Irwin. Discharge deposits that formed in areas of paleodischarge consist of fine-grained sediments that commonly exhibit mottled dark and light colors, indicative of wetting and drying cycles, and form raised mounds or platforms. They are generally loose and fine grained, similar to active discharge deposits, but in some cases include dense crystalline rock such as travertine. Inactive discharge deposits are generally dry and thus have extremely sparse vegetation. Discharge deposits may host archeological sites (for example, Hall, 1994; Basgall, 1994) and carry vital information about present and past levels of the water table (for example, Quade and others, 1995; Pigati and others, 2011).

Soil Development

Understanding soil development in surficial deposits is vital because it dramatically changes the permeability and storage capacity of sediment for water (McDonald and others, 1995; Hamerlynck and others, 2002; Miller and others, 2009). Soil development begins when the surface of a deposit is stabilized. The development of soil can be described by a series of progressive changes to the sediment that proceed apace with several changes to the deposit's surface morphology (described as micro-relief) and several other indicators such as pavement development and varnish accumulation on surface clasts. All of these changes together describe a path of progressive changes that are correlated with the age of the deposit (McFadden and others, 1989). As a result, we describe the soil development below in a framework of age of deposit or soil chronosequence. Fundamental contributions to the development of desert soil chronosequences in the eastern Mojave Desert are McFadden and others (1989), Reheis and others (1989), and McDonald and others (1995).

In general, soil development proceeds with the addition of silt and very fine sand to the sediment resulting from infiltration of wind-blown materials. The silt and sand collect just below a gravel pavement as a vesicular A horizon (Av), infiltrates deeper to contribute to an oxidized, sometimes clayey B horizon, and deeper yet, contributes $CaCO_3$ to the profile to develop a calcic horizon (Bk). Added materials are primarily in the size range from fine sand to clay. As a result of added eolian materials in swales and local redistribution of materials by sheetflow, surface microrelief tends to decrease with time until a nearly flat surface results, after which dissection progressively fragments the flat surfaces to form rounded elongate ridges. Varnish of surface clasts and desert pavement development increase with time until surfaces start to degrade owing to dissection. McFadden and others (1989) showed that varnish accumulation and soil development are the two most diagnostic parameters for deposit age. Within restricted environments, other parameters are also useful. Soil and surface features are summarized in table 1 and described in the following paragraphs.

Young deposits (Qy).—Surfaces undergoing active deposition generally exhibit little or no soil development. As a result, active parts of alluvial fans are made up of coarse gravelly sand with few fines. Young surfaces that are mostly stabilized and receiving only extremely infrequent inundations by water carrying sediment or by blowing sand begin to develop soil horizons such as weak, sandy Av horizons and weak cambic (Bw) horizons. Surfaces typically armor with gravel by one or more of the following processes: (1) wind erosion removing fine particles to create a gravel layer (weak regolith), (2) weak desert pavement formed by pebbles floating on an Av horizon, (3) mineralogic crusts such as bound clay, and (4) biological soil crusts composed of cyanobacteria, lichens, and mosses. A surface armor greatly increases stability. Microrelief associated with depositional processes, such as bar and swale on alluvial fans, becomes progressively muted with time as swales gradually fill. The processes of infiltration of eolian fines, leading to soil horizonation, lead to progressive soil development in young deposits. This increase in fines, particularly in the Av horizon, reduces bulk infiltration rates (McDonald and others, 1995; Hamerlynck and others, 2002).

Intermediate-age deposits (Qi).—Surfaces reach maximum stability and begin to degrade during intermediate ages. Desert pavements, generally formed by tightly interlocked pebbles of nearly the same size that have uniform surface heights, a dark varnish of pebbles, and flat surfaces are hallmarks of intermediate-age alluvial fans. The surfaces generally are moderately to deeply incised with efficient water and sediment bypass in the incised channels. With progressive age of intermediate-age surfaces, morphology changes from weak remnant bar and swale, to flat, to crowned or rounded (Miller and others, 2009). Soil horizonation is at a maximum: strongly developed Av horizons are nearly entirely silt and clay mixtures and structured as platy, hard layers 5–15 cm thick; red Bt horizons may be hundreds of centimeters thick and clay rich; and calcic horizons (Gile and others, 1966; Machette, 1985) commonly reach stage II and III. The strongly developed Av horizon greatly impedes vertical infiltration (McDonald and others, 1995; Hamerlynck and others, 2002) and enhances surface run-off during precipitation events.

Old deposits (Qo).—Eroded landforms and stripped soil horizons mark old surfaces. Typical landforms are ballenas (whalebacks) that are rounded and 5–15 m above neighboring channels. Remnants of A and B horizons are uncommon, but calcic horizons are well developed as stage IV and greater, and constitute much of the exposed deposit. The calcic horizons contribute chips and chunks to surface litter and weak pavements, creating a light tone for many of the old deposits. The surface may exhibit a young or intermediate-age pavement that is superimposed on the degraded old deposit as a result of short-term stabilization. Old alluvial fan deposits are relatively well vegetated despite decreased infiltration caused by the advanced calcic horizon. Plants apparently take advantage of fracture permeability to capture sufficient moisture. Despite the deeply incised landforms of old alluvial deposits, the crests of ballenas generally define alluvial fan or piedmont morphology.

Very old deposits.—Deposits older than the old deposits typically do not conform to eroded landforms and display no pedogenic soils and few if any buried soils despite thick exposures. They are deeply dissected, sometimes forming badlands. In some cases the deposits appear to be out of context with present landforms; they grade to nonexistent source terranes or have clasts indicating source rocks that are not currently being supplied to the area. These very old deposits were described in the previous section on Pliocene and early Pleistocene deposits.

Faults and Folds

Structures such as faults and folds commonly cause basins to form and influence the geometry of the basins and the types of deposits in the basins. In addition, these structures can deform basin deposits and cause basins to become hydrologically compartmentalized. In this section of the report we describe the structures formed during the late Cenozoic in the Fort Irwin area in order to help elucidate hydrologic characteristics of the region.

Faults and the Formation of Basins

Faults in the Fort Irwin area include numerous northwest- and east-striking faults with lesser amounts of north- and northeast-striking faults, all of which are consistent with the deformation associated with the Eastern California Shear Zone (Dokka and Travis, 1990) and the older history of deformation associate with the Mojave Strike-Slip Province (Miller and Yount, 2002) (fig. 1). Many of these faults are associated with (dextral or sinistral) strike-slip, oblique-slip, or (normal or thrust) dip-slip separation (Miller and others, 2014). For example, (1) most northwest-striking faults have dextral separation, and a few have oblique separation, (2) most east-striking faults, including some west-to-northwest-striking faults, have sinistral separation, (3) many of the north- and northeast-striking faults have oblique separation, and most northwest- and northeast-striking faults located north of the Garlock Fault Zone have oblique separation, and (4) many of the west-to-northwest- and east-to-northeast-striking faults, especially those near the intersections of other fault zones, have thrust separation. Schemer and others (1996) and Miller and Yount (2002) describe faults in the Fort Irwin area that were active during the Miocene and Pliocene, and some are coincident with those active during the Quaternary, but typically they do not cut Holocene deposits (Miller and others, 2014).

The Fort Irwin region has experienced two tectonic regimes (one extensional, the other strike slip) during the late Cenozoic, the time when most basin deposits were formed and deformed. The earlier event was extensional but is poorly defined in Fort Irwin. South, north, and east of Fort Irwin, large-magnitude extension occurred and formed basins with generally coarse-grained, moderately to well-consolidated deposits. Extension in the area around Barstow, where it is associated with the Central Mojave metamorphic core complex of ~24–19 Ma age (Glazner and others, 2002), formed roughly 1-km-thick sedimentary basins and volcanic sequences including those in Alvord Mountain (Byers, 1960; Fillmore, 1993) and the northern

Table 1. Summary of principal characteristics for piedmont deposits of the central Mojave Desert (after Miller and others, 2009) and summarized by Miller and others (2014).

[Av, vesicular A horizon; B, B horizon; Bw, weak cambic; Bt, accumulated silicate clays; cm, centimeter; descriptions of Stage I, II, III, and IV are in Gile and others (1966), Machette (1985), and Miller and others (2009)]

Unit label	Surface topography	Pavement	Varnish	Av	B	Calcic morphology	Plants
Qya1	Active wash or fan	None	None	None	None	None	Few; *Hymenoclea salsola*
Qya2	Bar and swale strong	None	None to very weak	Generally none	None	None	*Hymenoclea salsola, Larrea tridentata, Ambrosia dumosa*
Qya3	Remnant bar and swale, somewhat flat	Incipient	Weak	Weak; sandy silt	Weak (Bw) reddish	Stage I	*Larrea tridentata, Ambrosia dumosa*
Qya4	Weak remnant bar and swale, fairly flat	Weak; some leveling of pebbles	Weak to moderate	Weak; sandy silt, loose	Bw	Stage I	*Larrea tridentata, Ambrosia dumosa*
Qia1	Flat, faint bar and swale	Weak to moderate	Moderate	Structured silt, 2–6 cm	Strong red, weak clay	Stage II	Sparse plants
Qia2	Flat, even pebble size, pebble tops level	Moderate to strong	Moderate to strong	Structured silt, 4–8 cm	Bt usually; moderate clay	Stage II to III	Sparse; *Yucca schidigera*
Qia3	Crowned	Strong to degraded; exposed Av	Strong; purplish casts	Structured silt, 4–15 cm	Bt; strong clay	Stage III to IV	Sparse
Qoa	Whaleback	Calcic chips in pavement	Secondary or none	Secondary or none	Secondary or none	Stage IV	Common plants, many species

Calico Mountains (McCulloh, 1965),but they are not known farther north in much of Fort Irwin. North of the Garlock Fault, a complex, commonly superposed system of Basin and Range extensional basins formed during roughly this same time (Monastero and others, 2002; Fridrich and Thompson, 2011), but these basins are not known in the Fort Irwin area south of the Garlock Fault Zone. Southwest of the Avawatz Mountains, a thick sedimentary basin fill described by Spencer (1990b) was attributed to extensional origins; the Miocene Avawatz Formation in this basin crops out along the eastern side of the Fort Irwin area. The basin deposits of this episode have been disrupted by later strike-slip faults and have no relation to modern basins, but they contribute to gravity-defined basin areas and may represent a source for groundwater.

As noted earlier (in the “Miocene Volcanic Sequence” and “Miocene Sedimentary Sequence” sections), the gravity interpretation of the Fort Irwin area (Jachens and Langenheim, 2014) forms a relatively complex set of small elongate basins beneath Nelson basin (with some segmentation possibly resulting from deformation near the Nelson Lake fault) that grade into a westward-deepening basin beneath the Eagle Crags area. It is important to note that for the central and western parts of the basin beneath the Eagle Crags area, based on the small number of gravity observations on outcrops and how the Cenozoic deposits and basement were modeled, deep basins are shown in the proper locations, and their boundaries are correct, but the exact depth to basement is uncertain (Jachens and Langenheim, 2014). However, the geometry of these basins, combined with the generally northwest-oriented belt of Miocene volcanic rocks (fig. 3), is reminiscent of extension-related basins of the Central Mojave metamorphic core complex, and may point to previously unrecognized extensional basins in western Fort Irwin.

Extensional tectonism was followed by a ~18–12 Ma successor basin phase, during which broad alluvial basins locally held lakes and formed the widespread Barstow, Spanish Canyon, and Hector Formations (Fillmore 1993; Miller and others 2010; Woodburne and Reynolds, 2010), and the informally named “Fort Irwin basin” of Pavlis and others (1998). These shallow basins of generally fine-grained, moderately consolidated rocks covered the southern part of the Fort Irwin area including the plain south of Coyote Lake, Alvord Mountain, and the area southwest of Bicycle Lake (Byers, 1960). Similar fluvial and lacustrine sediment accumulated in “Fort Irwin basin” west of and on rocks of the Avawatz Formation. This latter basin is poorly dated and is in part younger than the Barstow Formation based on 11–10 Ma tuffs in the fine sand to mud and evaporate sequence (Sobieraj, 1994; Schermer and others, 1996; Miller and Yount, 2002; Miller and others, 2010). A similar section to the “Fort Irwin basin” occurs in the Nelson Lake area, including being penetrated by NELT drillholes (described above in the “Miocene Sedimentary Sequence” sections), and might represent more deposits from this time interval. During this ~18–12 Ma time, much of the volcanic section in northwestern Fort Irwin accumulated, probably as an extensive constructional highland associated with the Eagle Crags volcanic field described by Sabin and others (1994), and based on the outcrop area of this volcanic field, it was not controlled by basin-bounding faults. Within the northern and western Avawatz Mountains, a slightly younger (middle to late Miocene) thick sequence of sedimentary fill of the Military Canyon Formation was deposited in narrow elongate fault-generated trough interpreted to possibly have formed within a Miocene phase of strike-slip faulting on a proto-Garlock Fault Zone (Brady and Troxel, 1999). This strike-slip faulting may have been kinematically linked with contemporaneous early phases of extension and basin formation in this area (Serpa and Pavlis, 1996; Guest and others, 2003; Fridrich and Thompson, 2011).

At a poorly defined time, probably after 11 Ma (Schermer and others, 1996), strike-slip faulting started in the Fort Irwin area as the Eastern California Shear Zone began to form. The zone translates part of the North American-Pacific Plate motion northward away from the southern San Andreas Fault (Dokka and Travis, 1990; Schermer and others, 1996) and across the central Mojave Desert. The strike-slip faulting continues to the present, and represents overall dextral shear across the central Mojave Desert, under an approximate north-south maximum principal stress. In the Fort Irwin area, two contrasting fault domains formed, one (in the west and east) consisting of the typical northwest-striking, dextral faults, and the other (covering a broad swath of the center) consisting of east-striking sinistral faults. Near the northern boundary of Fort Irwin, the Garlock Fault forms the northern margin of this sinistral domain, and the southern boundary lies well to the south of the Fort Irwin map area. These strike slip faults displaced and disrupted the extensional basin deposits.

Basins formed along dextral faults probably are associated with releasing stepovers in the faults that form elongate basins in regions of local extension. Examples include Goldstone Lake, where faults are poorly defined, the Red Pass basin, and the southwest part of the Riggs basin, where narrow step-overs in dextral faults are defined by gravity and magnetic patterns indicating narrow, deep basins (Jachens and Langenheim, 2014).

Basins that formed along sinistral faults appear to be more complicated than those associated with dextral faults, possibly because these faults are associated with rotating blocks and the faults may change from extensional to compressive behavior with time. Basins that formed in stepovers may be present in places such as the Nelson basin area, where ridges and hills represent push-ups of the basin materials, demonstrating the contrasting extension and compression along these faults. These types of along fault transitions from extension to compression are also depicted in the elongate thicker and thinner parts of the depth to basement map in the Nelson basin area (Jachens and Langenheim, 2014). The modern physiography of east-oriented elongate basins, many with basin axes on the south sides against steep mountain fronts (Miller and Yount, 2002), suggests that sediment accumulation in the broad valleys was potentially significant. However, most of the modern valleys are externally drained and some earlier basins were also probably externally drained (Miller and others, 2011), so little sediment probably accumulated. Leach Lake, which contains fault-parallel, elongate, thicker and thinner depths of folded sediment and sedimentary rocks (Bedrosian and others, 2014; Jachens and Langenheim, 2014), may be an exception, as it is a very large internally drained basin today and perhaps in the past. In southern Fort Irwin, evidence from poorly consolidated Pliocene deposits 100–300 m thick indicates eastward flowing rivers were sourced in highlands near Goldstone Mining District; therefore, valleys similar to current valleys were present longer than 4 million years. Importantly for the hydrogeology, the sediment shed into these valleys is coarse grained in the west and much finer in the east.

Basins that formed in complex junctions between east-striking sinistral and northwest-striking dextral faults are the most common basins in the Fort Irwin area. Many of these junctions include a third, north-northwest-oriented fault set that plays an enigmatic role in the fault interactions. These faults appear to be oblique-dextral slip, with normal and reverse components of slip. Near several of these north-striking faults are small basins (Langford, Bicycle) as well as complexes of many closely spaced faults. Thrust faults are present in a few places, such as east of Bicycle Lake playa and east of the Avawatz Mountains. Red Pass basin may have formed in one of these complex junctions, but it also coincides with the Miocene “Fort Irwin basin” and therefore its gravity-defined extent may not be caused strictly by young faults. Cronese basin probably resulted from interactions among the Coyote Lake and Bicycle Lake sinistral faults and the dextral Soda Mountain Fault, but basin-fill exposures are sparse.

Several other styles of basins have formed along and north of the eastern Garlock Fault Zone in the northern map area. The Garlock Fault Zone in this area is approximately located along or adjacent to the northern boundaries of several east-trending irregular alluvial basins that occupy lowland areas, including Leach Lake playa and the Denning Springs area between the Granite Mountains on the south and the western Avawatz Mountains on the north. Specifically, from west to east, the fault zone follows the southern margin and adjacent piedmont of the southwestern Owlshead Mountains, cuts across Leach Lake playa in the interior of the western basin, obliquely transects the southwestern flank of the Avawatz Mountains, and complexly traverses the northern margin of the Avawatz Mountains. These basins appear to have formed in response to several intervals of deformation. The southern margins are mostly pedimented and were structurally defined by an older set of mostly inactive thrust faults that do not deform middle Quaternary surficial deposits, although locally the boundary follows a set of northwest-trending right-lateral faults with mid-late Quaternary activity. The northern margins of the basins are structurally defined by active components of the eastern Garlock Fault, including either major translational strands or blind thrusts associated with transpressive uplift along the fault zone. An additional narrow restricted zone of subsidence in the center of Leach Lake playa developed on a pull-apart graben associated with a transtensional stepover zone in the core of two translational strands of the Garlock Fault Zone.

Folds

Folds are widely present in Fort Irwin and can be found at many scales, but the most important folds for basin formation in the area south of the Garlock Fault are limited to two places; Superior and Coyote basins. Elsewhere, folds have deformed basin sediment, and this might contribute to complex basin hydrology (for example, pop-up hills and folds in Nelson Lake basin, and folded Miocene sandstone and siltstone northeast of the Tiefort Mountains [Pavlis and others, 1998]).

At Superior basin, one or two dextral faults lie east of the basin and the Blackwater Fault lies west of it (Amoroso and Miller, 2012). However, these faults appear to have no relation to the basin, which lies in a downwarp or sag between two large tilted landscapes, including the northward sloping Coolgardie plateau to the south and the southward sloping southern margin of the Eagle Crags volcanic field to the north (fig. 1). The topography and location of the modern Superior Lakes playas suggest that this downwarping is modern, but the depth of the basins and the degree that they are bounded by faults are not known from geologic map information. Gravity data led Jachens and Langenheim (2014) to the interpretation that a broad, west-northwest, moderate-depth basin exists just north of the Superior Lakes. The deepest part of the west-northwest basin appears to coincide with a north-trending belt of Miocene volcanic rocks located east of the area underlain by the 3.8 Ma Black Mountains basalt, and these volcanic rocks might accentuate the apparent depth of sediment in the basin.

Coyote basin represents a downwarped area of the tectonic block bounded on the south by the Cave Mountain Fault and on the north by the Coyote Lake Fault. In this case, much or all of the downwarping occurred during the late Pliocene to Quaternary (Miller and Yount, 2002; Miller and others, 2011) and probably was caused by bending of that tectonic block resulting in a ‘wrinkle’ or downwarp. The deformation of the block might be influenced by end effects from vertical-axis rotation of the block, the westward convergence of the Cave Mountain and Coyote Lake Faults, interaction with the Paradise Fault, or as mentioned by Miller and others (2011), a complex interaction of numerous smaller intra-block faults. Basin fill is not exposed, and thicknesses estimated from gravity data (Jachens and Langenheim, 2014) of as much as 1 km probably include Miocene strata as well as those of Pliocene to Quaternary age. The Miocene Barstow Formation is exposed in nearby pop-up hills, overlain by Pliocene gravel about 100 m thick in most cases.

Active folding at several scales is also an important factor in the formation of many alluvial basins in the area north of the Garlock Fault Zone. At a regional scale, the main axial trough of southern Death Valley to the north of the Avawatz Mountains has formed in response to active synclinal downwarping to the north of the frontal thrust faults of the northeastern Avawatz Mountains and Southern Death Valley Fault Zone. This downwarping is indicated by the prevalence of thrust faults and associated fault-related folding along most of the range fronts of the Avawatz and southern Owlshead Mountains that define the southern and western structural boundaries of this basin. Miller and others (2014; in their fig. 1 and map sheet) document many of the thrust systems, and similar systems have been identified and mapped along the continuation of the western basin boundary to the northwest of the map area. A number of additional smaller scale pop-up folds and thrust faults have been mapped in the area, which are not shown on these more generalized figures. The prevalence of the contractional structures along the main range-front bounding southern Death Valley contrasts with the complete absence of major range-front normal faults at the surface along these basin boundaries. Further, geophysical modeling of geophysical surveys in southern Death Valley provide no evidence for deep buried fault-bounded grabens or half-grabens indicative of major extensional subsidence in the basin interior (for example, Blakely and others, 1999). Rather, these studies indicate thin accumulation of alluvial fill above a shallow-depth bedrock trough consistent with observed topography and surficial depositional patterns in this basin. Thus, the southern part of the Death Valley basin system appears to reflect contractional downwarping rather than the extensional subsidence on half-grabens characteristic of the main basins to the north. There is additional smaller scale basin modification related to synformal downwarping between adjacent anticlinal uplift that entraps local sedimentation on basin margins and embayments north of the Leach Lake playa and between the northwestern Avawatz and southeastern Owlshead Mountains.

Conclusions

During the Miocene, the area of Fort Irwin consisted of numerous basins that accumulated epiclastic sandstone and conglomerate as volcanic fields north of the Garlock Fault and at Eagle Crags built high tablelands. Along the eastern margin of the Eagle Crags volcanic field, a series of lava flows, associated pyroclastic deposits, and volcaniclastic sediments was deposited in alluvial, fluvial, and locally lacustrine environments that created an intricate three-dimensional volcanic architecture. In the eastern part of Fort Irwin, mostly epiclastic sediments with locally interstratified tuffs were deposited in alluvial, fluvial, and possibly lacustrine environments. Upper Miocene to Pliocene rocks are either poorly represented or not identified in western Fort Irwin, but in eastern Fort Irwin there are (1) a 11.65±0.13 Ma waterlain tuff near the top of a sequence of distal fan and lacustrine deposits, (2) megabreccia (landslide) deposits that overlie ~10 Ma fluvial and lacustrine deposits, and (3) the ~5.6 Ma Bicycle Lake basalt. Throughout the latest Pliocene and Quaternary, sandstone and conglomerate were deposited in alluvial and fluvial environments, and locally fine-grained sediments were deposited in lacustrine, playa, eolian, and groundwater discharge environments.

The Fort Irwin area is transected by Neogene to Holocene northwest- and east-striking (and fewer northeast-striking) strike-slip, normal, and locally thrust faults, and many of the structural blocks between faults are broadly warped where rocks adjacent to the faults are folded and sheared. In western Fort Irwin, most Miocene volcanic and sedimentary sequences are conformable (or form buttress unconformities), and in many areas, the stratigraphic section is deformed into broad homoclines, or large synclinal folds that formed some of the larger depositional basins. In eastern Fort Irwin, many of the Miocene sedimentary sequences are bounded by angular unconformities that indicate deformation by folding or faulting. Many northwest-, northeast-, east-striking, and local thrust faults form discrete fractures or scarps, and some result in folds and flower structures. Basins have formed along, or at the intersections of, all four types of faults. Schermer and others (1996) demonstrated that activity on many faults, especially the east-striking faults, began about 11 Ma and interpreted this as the inception of the Eastern California Shear Zone in this part of the Mojave region. Many faults in the Fort Irwin area were active into the mid-Quaternary, and do not cut Holocene deposits. The few faults active during the Holocene include the Garlock Fault and several fault systems around the periphery of the central Fort Irwin area (such as the Owlshead Lake Fault and the East Goldstone Lake Fault in western Fort Irwin).

In the Fort Irwin area, the late Cenozoic (Neogene, and mostly Miocene) volcanic and sedimentary facies and associated faults form a three-dimensional stratigraphic architecture that define the vertical and lateral continuity of rocks. The continuity or spatial limitations of rocks constrain the distribution of lithologic and hydrogeologic properties important for many hydrogeologic processes. During the late Miocene and Quaternary, continued sedimentation and the deformation of the stratigraphic architecture further influenced how water moved (and moves) through the hydrogeologic system. Thus, the unique geologic history of each basin provides a geologic framework for groundwater resources.

References Cited

Amoroso, L., and Miller, D.M., 2012, Surficial geologic map of the Cuddeback Lake 30’ x 60’ quadrangle, San Bernardino and Kern Counties, California: U.S. Geological Survey Scientific Investigations Map 3107, pamphlet 31 p., 1 sheet, 1:100,000 scale, https://pubs/usgs/gov/sim/3107.

Barton, N., and Choubey, V., 1977, The shear strength of rock joints in theory and practice: Rock Mechanics, v. 10, no. 1–2, p. 1–54.

Basgall, M.E., 1994, Deception knoll (CA-SBR-5047)—An early Holocene encampment in the north-central Mojave Desert, California, *in* Reynolds, R.E., ed., Off limits in the Mojave Desert: San Bernardino County Museum Association Special Publication 94-1, p. 61–70.

Bedrosian, P.A., Ball, L.B., and Bloss, B.R., 2014, Airborne electromagnetic data and processing within Leach Lake Basin, Fort Irwin, California, chap. G of Buesch, D.C., ed., Geology and geophysics applied to groundwater hydrology at Fort Irwin, California: U.S. Geological Survey Open-File Report 2013–1024–G, 20 p., https://doi.org/10.3133/ofr20131024G.

Blakely, R.J., Jachens, R.C, Calzia, J.P., and Langenheim, V.E., 1999, Cenozoic basins of the Death Valley extended terrane as reflected in regional-scale gravity anomalies, *in* Wright, L.A, and Troxel, B.W., eds., Cenozoic Basins of the Death Valley Region: Boulder, Colorado, Geological Society of America Special Paper 333, p. 116.

Bloss, B.R., and Bedrosian, P.A, 2015, Laboratory electrical resistivity analysis of geologic samples from Fort Irwin, California, chap. E *of* Buesch, D.C., ed., Geology and geophysics applied to groundwater hydrology at Fort Irwin, California: U.S. Geological Survey Open-File Report 2013–1024–E, 104 p., https://doi.org/10.3133/ofr20131024E.

Brady, R.H., III, 1984, Neogene stratigraphy of the Avawatz Mountains between the Garlock and Death Valley fault zones, southern Death Valley, California—Implications as to late Cenozoic tectonism: Sedimentary Geology, v. 38, no. 1–4, p. 127–157.

Brady, R.H., III, 1986a, Cenozoic geology of the northeastern Avawatz Mountains in relation to the intersection of the Garlock and Death Valley fault zones, San Bernardino County, California: Davis, Calif., University of California, Davis, Ph.D. dissertation, 292 p.

Brady, R.H., III, 1986b, Stratigraphy and tectonics of the northern Avawatz Mountains at the intersection of the Garlock and Death Valley fault zones, San Bernardino County, California, *in* Troxel, B.W., ed., Quaternary tectonics of southern Death Valley, California—Field trip guide: Shoshone, Calif., Friends of the Pleistocene Pacific Cell, p. 1–12.

Brady, R.H., III, and Troxel, B.W., 1999, The Miocene Military Canyon Formation—Depocenter evolution and constraints on lateral faulting, southern Death Valley, California, *in* Wright, L.A., and Troxel, B.W., eds., Cenozoic Basins of the Death Valley Region: Geological Society of America Special Paper 333, p. 277–288.

Buesch, D.C., 2006, Geologic evidence for limited ground motion damage in the Topopah Spring Tuff, Yucca Mountain, Nevada, *in* Hanks, T.C., Abrahamson, N.A., Board, M., Boore, D.M., Brune, J.N., and Cornell, C.A., eds., Report of the workshop on extreme ground motions at Yucca Mountain, August 23–25, 2004: U. S. Geological Survey Open-File Report 2006–1277, Appendix C, p. 1–9.

Buesch, D.C., 2012, Stratigraphy of the possible Peach Spring Tuff in the Alvord Mountain area, California, *in* Reynolds, R.E., ed., The 2012 desert symposium field guide and proceedings: California State University Desert Studies Consortium, p. 179–180.

Buesch, D.C., 2014, Introduction to the geologic and geophysical studies of Fort Irwin, California, chap. A *of* Buesch, D.C., ed., Geology and geophysics applied to groundwater hydrology at Fort Irwin, California: U.S. Geological Survey Open-File Report 2013–1024–A, 8 p., https://doi.org/10.3133/ofr20131024A.

Buesch, D.C., 2018, Lithostratigraphic framework in boreholes from Goldstone Lake and Nelson Lake basins, Fort Irwin, California, chap. D *of* Buesch, D.C., ed., Geology and geophysics applied to groundwater hydrology at Fort Irwin, California: U.S. Geological Survey Open-File Report 2013–1024–D, 131 p., https://doi.org/10/3133/ofr20131024D.

Buesch, D.C., Beason, S.C., and Spengler, R.W., 1999, Relations among welding, vapor-phase activity, crystallization, and fractures in the Tiva Canyon and Topopah Spring Tuffs at Yucca Mountain, Nevada [abs.]: Geological Society of America Abstracts with Programs, v. 31, no. 7, p. A476–A477.

Buesch, D.C., Spengler, R.W., Moyer, T.C., and Geslin, J.K., 1996, Proposed stratigraphic nomenclature and macroscopic identification of lithostratigraphic units of the Paintbrush Group exposed at Yucca Mountain, Nevada: U.S. Geological Survey Open-File Report 94–469, 47 p., https://pubs.er.usgs.gov/publication/ofr94469.

Buesch, D.C., Miller, D.M., and Hillhouse, J.W., 2013, Lithology, age, and paleomagnetic characteristics of the lower tuffaceous sequence in the Spanish Canyon Formation, Alvord Mountain, California, *in* Reynolds, R.E., ed., The 2013 Desert Symposium Field Guide and Proceedings: California State University Desert Studies Consortium, 227 p.

Burgess, M.K., and Bedrosian, P.A., 2014, Time-domain electromagnetic surveys at Fort Irwin, San Bernardino County, California, 2010–12, chap. F *of* Buesch, D.C., ed., Geology and geophysics applied to groundwater hydrology at Fort Irwin, California: U.S. Geological Survey Open-File Report 2013–1024–F, 64 p., https://doi.org/10.3133/ofr20131024F.

Byers, F.M., 1960, Geology of the Alvord Mountain quadrangle, San Bernardino County, California: U.S. Geological Survey Bulletin 1089–A, 71 p., https://pubs.er.usgs.gov/publication/b1089A.

Dibblee, T.W., and Minch, J.A, 2008, Geologic map of the Opal Mountain & Lane Mountain 15 minute quadrangles, San Bernardino County, California: Santa Barbara, Calif., Dibblee Geologic Foundation Map DF-403, scale 1:62,500.

Dokka, R.K., and Travis, C.J., 1990, Role of the eastern California shear zone in accommodating Pacific-North American plate motion: Geophysical Research Letters, v. 17, no. 9, p. 1323–1326.

Ferguson, C.A., McIntosh, W.C., and Miller, C.F., 2013, Silver Creek caldera—The tectonically dismembered source of the Peach Spring Tuff: Geology, v. 41, no. 1, p. 3–6, https://doi.org/10.1130/G33551.1.

Fillmore, R.P., 1993, Sedimentation and extensional basin evolution in a Miocene metamorphic core complex setting, Alvord Mountain, central Mojave Desert, California, USA: Sedimentology, v. 40, no. 4, p. 721–742.

Flint, A.L., Flint, L.E., Kwicklis, E.M., Bodvarsson, G.S., and Fabryka-Martin, J.M., 2001, Hydrology of Yucca Mountain, Nevada: Reviews of Geophysics, v. 39, no. 4, p. 447–470, https://doi.org/10.1029/1999RG000075.

Flint, A.L., Flint, L.E., Kwicklis, E.M., Fabryka-Martin, J.T., and Bodvarsson, G.S., 2002, Estimating recharge at Yucca Mountain, Nevada, USA—Comparison of methods: Hydrogeology Journal, v. 10, no. 1, p. 180–204, https://doi.org/10.1007/s10040-001-0169-1.

Flint, L.E., Buesch, D.C., and Flint, A.L., 2006, Characterization of unsaturated zone hydrogeologic units using matrix properties and depositional history in a complex volcanic environment: Vadose Zone Journal, v. 5, no. 1, p. 480–492.

Ford, J.P., MacConnell, D.F., and Dokka, R.K., 1992, Neogene faulting in the Goldstone-Fort Irwin area, California—A progress report, *in* Richard, S.M., ed., Deformation associated with the Neogene eastern California shear zone, southeastern California and southwestern Arizona: San Bernardino County Museum Association Special Publication 92–1, 32 p.

Fridrich, C.J., and Thompson, R.A., 2011, Cenozoic tectonic reorganizations of the Death Valley region, southeast California and southwest Nevada: U.S. Geological Survey Professional Paper 1783, 36 p., 1 plate, https://pubs.er.usgs.gov/publication/pp1783.

Gile, L.H., Peterson, F.F., and Grossman, R.B., 1966, Morphological and genetic sequences of carbonate accumulation in desert soils: Soil Science, v. 101, no. 5, p. 347–360.

Glazner, A.F., Walker, J.D., Bartley, J.M., and Fletcher, J.M., 2002, Cenozoic evolution of the Mojave block of southern California, *in* Glazner, A.F., Walker, J.D., and Bartley, J.M., eds., Geologic evolution of the Mojave Desert and southwestern Basin and Range: Geological Society of America Memoir 195, p. 19–41.

Green, H.L, 2009, Neotectonic investigation of the southern Death Valley fault zone, southeastern California: San Francisco, Calif., San Francisco State University, M.S. thesis, 133 p., scale 1:12,000.

Grose, L.T., 1959, Structure and petrology of the northeast part of the Soda Mountains, San Bernardino County, California: Geological Society of America Bulletin, v. 70, no. 12, p. 1,509–1,548.

Guest, B., Pavlis, T.L., Golding, H., and Serpa, L., 2003, Chasing the Garlock—A study of tectonic response to vertical axis rotation: Geology, v. 31, no. 6, p. 553–556.

Hall, M.C., 1994, Middle Holocene human occupation site CA-SBR-5251 in Tiefort basin, Fort Irwin, San Bernardino County, California: San Bernardino County Museum Association Special Publication 94-1, p. 71–80.

Hamerlynck, E.P., McAuliffe, J.R., McDonald, E.V., and Smith, S.D., 2002, Ecological responses of two Mojave Desert shrubs to soil horizon development and soil water dynamics: Ecology, v. 83, no. 3, p. 768–779.

Harden, J.W., and Taylor, E.M., 1983, A quantitative comparison of soil development in four climatic regimes: Quaternary Research, v. 20, no. 3, p. 342–259.

Jachens, R.C., and Langenheim, V.E., 2014, Gravity survey and interpretation of Fort Irwin and vicinity, Mojave Desert, California, chap. H *of* Buesch, D.C., ed., Geology and geophysics applied to groundwater hydrology at Fort Irwin, California: U.S. Geological Survey Open-File Report 2013–1024–H, 11 p., https://doi.org/10.3133/ofr20131024H.

Jennings, C.W., 1994, Fault activity map of California and adjacent areas: California Division of Mines and Geology Geologic Data Map No. 6, scale 1:750,000.

Jennings, C.W., Burnett, J.L., Troxell, B.W., 1962, Geologic map of the Trona sheet, California: California Division of Mines and Geology, scale 1: 250,000.

Kjos, A.R., Densmore, J.N., Nawikas, J.M., and Brown, A.A., 2014, Construction, water-level, and water-quality data for multiple-well monitoring sites and test wells, Fort Irwin National Training Center, San Bernardino County, California, 2009–12: U.S. Geological Survey Data Series 788, 139 p., https://doi.org/10.3133/ds788.

Langenheim, V.E., and Jachens, R.C., 2014, Aeromagnetic data, processing, and maps of Fort Irwin and vicinity, California, chap. I *of* Buesch, D.C., ed., Geology and geophysics applied to groundwater hydrology at Fort Irwin, California: U.S. Geological Survey Open-File Report 2013–1024–I, 18 p., https://doi.org/10.3133/ofr20131024I.

Luckow, H.G., Pavlis, T.L., Serpa, L.F., Guest, B., Wagner, D.L., Snee, L., Hensley, T.M., and Korjenkov, A., 2005, Late Cenozoic sedimentation and volcanism during transtensional deformation in Wingate Wash and the Owlshead Mountains, Death Valley: Earth Sciences Review, v. 73, no. 1–4, p. 177–219.

Machette, M.N., 1985, Calcic soils of the southwestern United States, *in* Weide, D.L., and Faber, M.L., eds., Soils and Quaternary geology of the southwestern United States: Geological Society of America Special Paper 203, p. 1–21.

MacConnell, D.F., McCabe, C., Dokka, R.K., and Chu, M., 1994, Paleomagnetic and structural evidence for localized tectonic rotation associated with fault drag in the northeastern Mojave Desert—Implications for the late Cenozoic tectonic evolution of Eastern California shear zone: Earth and Planetary Science Letters, v. 126, no. 4, p. 207–216.

McCulloh, T.H., 1960, Geologic map of the Lane Mountain quadrangle, California: U.S. Geological Survey Open-File Report 60-95, scale 1:48,000.

McCulloh, T.H., 1965, Geologic map of the Nebo and Yermo quadrangles, San Bernardino County, California: U.S. Geological Survey Open-File Report 65-107, scale 1:24,000.

McDonald, E.V., McFadden, L.D., and Wells, S.G., 1995, The relative influence of climatic change, desert dust, and lithologic control on soil-geomorphic processes on alluvial fans, Mojave Desert, California—Summary of results: San Bernardino County Museum Association Quarterly, v. 42, no. 2, p. 35–72.

McFadden, L.D., Ritter, J.B., and Wells, S.G., 1989, Use of multiparameter relative-age methods for age estimation and correlation of alluvial fan surfaces on a desert piedmont, eastern Mojave Desert, California: Quaternary Research, v. 32, no. 3, p. 276–290.

Menges, C.M., Taylor, E.M., Workman, J.B., and Jayko, A.S., 2001, Regional surficial-deposit mapping in the Death Valley area of California and Nevada in support of ground-water modeling, *in* Machette, M.N., Johnson, M.L., and Slate, J.L, eds., Quaternary and late Pliocene geology of the Death Valley region—Recent observations on tectonics, stratigraphy, and lake cycles (Guidebook for the 2001 Pacific Cell—Friends of the Pleistocene Field Trip): U.S. Geological Survey Open-File Report 01–51, p. H151–H166, https://pubs.er.usgs.gov/publication/ofr0151.

Miller, D.M., 2012, Surficial geologic map of the Ivanpah 30' x 60' quadrangle, San Bernardino County, California, and Clark County, Nevada: U.S. Geological Survey Scientific Investigations Map 3206 pamphlet, 14 p., 1 sheet, scale 1:100,000.

Miller, D.M., Bedford, D.R, Hughson, D.L., McDonald, E.V., Robinson, S.E., Schmidt, K.M., 2009, Mapping Mojave Desert ecosystem properties with surficial geology, *in* Webb, R.H., Fenstermaker, L.F., Heaton, J.S., Hughson, D.L., McDonald, E.V., and Miller, D.M., eds., The Mojave Desert, ecosystem processes and sustainability: Reno, Nev., University of Nevada Press, p. 225–251.

Miller, D.M., Leslie, S.R., Hillhouse, J.W., Wooden, J.L., Vazquez, J.A., and Reynolds, R.E., 2010, Reconnaissance geochronology of tuffs in the Miocene Barstow Formation—Implications for basin evolution and tectonics in the central Mojave Desert, *in* Reynolds, R.E., and Miller, D.M., eds., Overboard in the Mojave: Desert Studies Consortium, California State University, Fullerton, p. 70–84.

Miller, D.M., Reheis, M.C., Wan, E., Wahl, D.B., and Olson, H., 2011, Pliocene and early Pleistocene paleogeography of the Coyote Lake and Alvord Mountain area, Mojave Desert, California, *in* Reynolds, R.E., ed., The incredible shrinking Pliocene: Desert Studies Consortium, California State University, Fullerton, p. 53–67.

Miller, D.M., Menges, C.M., and Lidke, D.J., 2014, Generalized surficial geologic map of the Fort Irwin area, San Bernardino County, California, chap. B *of* Buesch, D.C., ed., Geology and geophysics applied to groundwater hydrology at Fort Irwin, California: U.S. Geological Survey Open-File Report 2013–1024–B, 11 p., scale 1:100,000, https://doi.org/10.3133/ofr20131024B.

Miller, D.M., and Yount, J.L., 2002, Late Cenozoic tectonic evolution of the north-central Mojave Desert inferred from fault history and physiographic evolution of the Fort Irwin area, California, *in* Glazner, A.F., Walker, J.D., and Bartley, J.M., eds., Geologic evolution of the Mojave Desert and southwestern basin and range: Geological Society of America Memoir 195, p. 173–197.

Miller, E.L., and Sutter, J.S., 1982, Structural geology and $^{40}Ar/^{39}Ar$ geochronology of the Goldstone-Lane Mountain area, Mojave Desert, California: Geological Society of America Bulletin, v. 93, p. 1,191–1,207.

Miller, J.S., Glazner, A.F., Walker, J.D., and Martin, M.W., 1995, Geochronologic and isotopic evidence for Triassic-Jurassic emplacement of the eugeoclinal allochthon in the Mojave Desert region, California: Geological Society of America Bulletin, v. 107, p. 1,441–1,457.

Miller, J.S., and Walker, J.D., 2002, Mesozoic geologic evolution of Alvord Mountain, central Mojave Desert, California, *in* Glazner, A.F., Walker, J.D., and Bartley, J.M., eds., Geologic evolution of the Mojave Desert and southwestern basin and range: Geological Society of America Memoir 195, p. 59–77.

Monastero, F.C., Walker, J.D., Katzenstein, A.M., and Sabin, A.E., 2002, Neogene evolution of the Indian Wells Valley, east-central California, *in* Glazner, A.F., Walker, J.D., and Bartley, J.M., eds., Geologic evolution of the Mojave Desert and southwestern basin and range: Geological Society of America Memoir 195, p. 199–228.

Oskin, M., and Iriondo, A. 2004, Large-magnitude transient strain accumulation on the Blackwater fault, eastern California shear zone: Geology, v. 32, no. 4, p. 313–316.

Pavlis, T.L., Serpa, L., Troxel, B., Dean, M., Hartman, T, and Rodosta, T., 1998, Late Cenozoic deformation in eastern Fort Irwin and its significance for the tectonic history of the Garlock fault system: San Bernardino County Museum Association Quarterly, v. 45, no. 2, p. 77–83.

Pigati, J.S., Miller, D.M., Bright, J.E., Mahan, S.A., Nekola, J.C., and Paces, J.B., 2011, Chronology, sedimentology, and microfauna of groundwater discharge deposits in the central Mojave Desert, Valley Wells, California: Geological Society of America Bulletin, v. 123, no. 11–12, p. 2,224–2,239, https://doi.org/10.1130/B30357.1.

Quade, J., Mifflin, M.D., Pratt, W.L., McCoy, W., and Burckle, L., 1995, Fossil spring deposits in the southern Great Basin and their implications for changes in water-table levels near Yucca Mountain, Nevada, during Quaternary time: Geological Society of America Bulletin, v. 107, no. 2, p. 213–230.

Reheis, M.C., Shroba, R.R., Harden, J.W., and McFadden, L.D., 1989, Development rates of late Quaternary soils, Silver Lake Playa, California: Soil Science Society of America Journal, v. 53, no. 4, p. 1,127–1,140.

Sabin, A. E., 1994, Geology of the Eagle Crags volcanic field, northern Mojave Desert, China Lake Naval Air Weapons Station, California: Golden, Colo., Colorado School of Mines, Department of Geology and Geological Engineering, Ph.D. dissertation, 190 p.

Sabin, A.E., Monastero, F.C., and Katzenstein, A.M., 1994, Middle to late Miocene age stratovolcano on the South Ranges, Naval Air Weapons Station, San Bernardino County, California, *in* McGill, S.F., and Ross, T.M., eds., Geological Investigations of an active margin: San Bernardino, Calif., San Bernardino County Museum Association, p. 293–301.

Schermer, E.R., and Busby, C.J., 1994, Jurassic magmatism in the central Mojave Desert—Implications for arc paleogeography and preservation of continental volcanic sequences: Geological Society of America Bulletin, v. 106, no. 6, p. 767–790.

Schermer, E.R., Luyendyk, B.P., and Cisowski, S., 1996, Late Cenozoic structure and tectonics of the northern Mojave Desert: Tectonics, v. 15, no. 5, p. 905–932.

Schermer, E.R., Stephens, K.A., Walker, J.D., 2001, Paleogeographic and tectonic implications of the geology of the Tiefort Mountains, northern Mojave Desert: Geological Society of America Bulletin, v. 113, no. 7, p. 920–938.

Serpa, L, and Pavlis, T.L., 1996, Three-dimensional model of the late Cenozoic history of the Death Valley region, southeastern California: Tectonics, v. 15, no. 6, p. 1,113–1,128.

Sobieraj, J.A., 1994, Sedimentology and tectonics of Tertiary fan deposits, Fort Irwin, northern Mojave Desert: Bellingham, Wash., Western Washington University, M.S. thesis, 111 p.

Spencer, J.E., 1990a, Geologic map of the southern Avawatz Mountains, northeastern Mojave Desert region, San Bernardino County, California: U.S. Geological Survey Miscellaneous Field Studies Map MF–2117, scale 1:24,000, https://pubs.er.usgs.gov/publication/mf2117.

Spencer, J.E., 1990b, Late Cenozoic extensional and compressional tectonism in the southern and western Avawatz Mountains, southeastern California, *in* Wernicke, B.P., ed., Basin and Range extensional tectonics near the latitude of Las Vegas, Nevada: Geological Society of America Memoir 176, p. 317–334.

Wagner, D.L., and Hsu, E.Y., 1987, Reconnaissance geologic map of parts of the Wingate Wash, Quail Mountains, and Manley Peak quadrangles, Inyo and San Bernardino Counties, southeastern California: California Division of Mines and Geology Open-File Report 87–10, scale 1:62,500.

Walker, J.D., Martin, M.W., Bartley, J.M., and Coleman, D.S., 1990, Timing and kinematics of deformation in the Cronese Hills, California, and implications for Mesozoic structure of the south-western Cordillera: Geology, v. 18, no. 6, p. 554–557.

Walker, J.D., Martin, M.W., and Glazner, A.F., 2002, Late Paleozoic to Mesozoic development of the Mojave Desert and environs, California, *in* Glazner, A.F., Walker, J.D., and Bartley, J.M., eds., Geologic evolution of the Mojave Desert and southwestern Basin and Range: Geological Society of America Memoir 195, p. 1–18.

Woodburne, M.O., and Reynolds, R.E., 2010, The mammalian litho- and biochronology of the Mojave Desert Province, *in* Reynolds, R.E., and Miller, D.M., ed., Overboard in the Mojave: Desert Studies Consortium, California State University, Fullerton, p. 124–147.

Workman, J.B., Menges, C.M., Page, W.R., Taylor, E.M., Ekren, E.B., Rowley, P.D., Dixon, G.L., Thompson, R.A., and Wright, L.A., 2002, Geologic map of the Death Valley ground-water model area, Nevada and California: U.S. Geological Survey Miscellaneous Field Studies MF-2381-A, pamphlet 47 p., 2 sheets, scale 1:250,000, https://pubs.er.usgs.gov/publication/mf2381A.

Wyatt, B.R., 2005, Plio-Pleistocene deformation at Alvord Mountain, central Mojave Desert, California: San Jose, Calif., San Jose State University, M.S. thesis, 66 p.

Yount, J.C., Schermer, E.R., Felger, T.J., Miller, D.M., and Stephens, K.A., 1994, Preliminary geologic map of Fort Irwin Basin, north-central Mojave Desert, California: U.S. Geological Survey Open-File Report 94–173, pamphlet 27 p., 1 sheet, scale 1:24,000, https://pubs.er.usgs.gov/publication/ofr94173.

ISSN 2331-1258 (online)
https://doi.org/10.3133/ofr20131024C